Article

Spatial Prioritization for Wildfire Mitigation by Integrating Heterogeneous Spatial Data: A New Multi-Dimensional Approach for Tropical Rainforests

Anjar Dimara Sakti [1,2,3], Adam Irwansyah Fauzi [4,5,*], Wataru Takeuchi [6], Biswajeet Pradhan [7,8,9], Masaru Yarime [10,11], Cristina Vega-Garcia [12], Elprida Agustina [13], Dionisius Wibisono [3], Tania Septi Anggraini [1,2,3], Megawati Oktaviani Theodora [3,4], Desi Ramadhanti [3,4], Miqdad Fadhil Muhammad [3], Muhammad Aufaristama [14], Agung Mahadi Putra Perdana [4,5] and Ketut Wikantika [1,2]

[1] Remote Sensing and Geographic Information Sciences Research Group, Faculty of Earth Sciences and Technology, Institut Teknologi Bandung, Bandung 40132, Indonesia; anjards@gd.itb.ac.id (A.D.S.); taniasepti@students.itb.ac.id (T.S.A.); ketut@gd.itb.ac.id (K.W.)
[2] Center for Remote Sensing, Institut Teknologi Bandung, Bandung 40132, Indonesia
[3] Geospatial Institute for Sustainability Action, Bandung 40132, Indonesia; dionisius.amw@students.itb.ac.id (D.W.); megawati.23117092@student.itera.ac.id (M.O.T.); desi.23117090@student.itera.ac.id (D.R.); miqdadfadhil@students.itb.ac.id (M.F.M.)
[4] Department of Geomatics Engineering, Faculty of Regional and Infrastructure Technology, Institut Teknologi Sumatera, Lampung Selatan 35365, Indonesia; mahadi.putra@gt.itera.ac.id
[5] Research and Innovation Center for Geospatial Information Science, Institut Teknologi Sumatera, Lampung Selatan 35365, Indonesia
[6] Institute for Industrial Science, The University of Tokyo, Tokyo 153-8505, Japan; wataru@iis.u-tokyo.ac.jp
[7] Centre for Advanced Modelling and Geospatial Information Systems (CAMGIS), School of Civil and Environmental Engineering, Faculty of Engineering & IT, University of Technology Sydney, Sydney, NSW 2007, Australia; Biswajeet.Pradhan@uts.edu.au
[8] Center of Excellence for Climate Change Research, King Abdulaziz University, Jeddah 21589, Saudi Arabia
[9] Earth Observation Centre, Institute of Climate Change, Universiti Kebangsaan Malaysia (UKM), Bangi 43600, Selangor, Malaysia
[10] Division of Public Policy, The Hong Kong University of Science and Technology, Hong Kong SAR, China; yarime@ust.hk
[11] Graduate School of Public Policy, University of Tokyo, Tokyo 113-0033, Japan
[12] Department of Agricultural and Forest Engineering-JRU CTFC-AGROTECNIO, Universitat de Lleida, 25003 Lleida, Spain; cristina.vega@udl.cat
[13] Air and Waste Management Research Group, Faculty of Civil and Environmental Engineering, Institut Teknologi Bandung, Bandung 40132, Indonesia; elpridaagustina@itb.ac.id
[14] Department of Applied Earth Sciences, Faculty of Geo-Information Science and Earth Observation, University of Twente, Hengelosestraat 99, 7514AE Enschede, The Netherlands; m.aufaristama@utwente.nl
[*] Correspondence: adam.fauzi@gt.itera.ac.id

Abstract: Wildfires drive deforestation that causes various losses. Although many studies have used spatial approaches, a multi-dimensional analysis is required to determine priority areas for mitigation. This study identified priority areas for wildfire mitigation in Indonesia using a multi-dimensional approach including disaster, environmental, historical, and administrative parameters by integrating 20 types of multi-source spatial data. Spatial data were combined to produce susceptibility, carbon stock, and carbon emission models that form the basis for prioritization modelling. The developed priority model was compared with historical deforestation data. Legal aspects were evaluated for oil-palm plantations and mining with respect to their impact on wildfire mitigation. Results showed that 379,516 km^2 of forests in Indonesia belong to the high-priority category and most of these are located in Sumatra, Kalimantan, and North Maluku. Historical data suggest that 19.50% of priority areas for wildfire mitigation have experienced deforestation caused by wildfires over the last ten years. Based on legal aspects of land use, 5.2% and 3.9% of high-priority areas for wildfire mitigation are in oil palm and mining areas, respectively. These results can be used to support the determination of high-priority areas for the REDD+ program and the evaluation of land use policies.

1. Introduction

Forests play an essential role in maintaining a balance in the ecosystem. Forests can reduce air temperature, produce oxygen, store carbon dioxide, provide clean water supply, and prevent several natural disasters such as landslides and floods [1]. Vegetation in forests can reduce the accumulation of carbon in the atmosphere through photosynthesis, as it absorbs CO_2, breaks it down, and stores it in the form of biomass [2]. Forest ecosystems have higher biodiversity compared with other ecosystems [3]. The Intergovernmental Panel on Climate Change reports that deforestation and forest degradation account for 17% of global greenhouse gas emissions (GHGs) and they occurred at the rate of 100,000 km^2 per year between 2015–2020, contributing significantly to the loss of biodiversity [4,5]. Recent data from Global Forest Watch (GFW) show that Indonesia lost 94,800 km^2 of primary forests from 2002 to 2019 [5]. This figure is equivalent to 36% of Indonesia's forest cover lost concurrently during that period [6].

Wildfire is a forest deforestation driver that results in losses in various aspects. It causes significant organic matter removal, loss of nutrients, change of quantity and composition of small invertebrates, and deterioration of structure and porosity of soil [7]. It also increases the probability of further burning in the following years, as dead trees topple to the ground, open up forest to drying by sunlight, and build up the fuel load with an increase in fire-prone species [8].

Rising global temperatures and more frequent heatwaves and associated droughts increase the likelihood of wildfire by promoting hot and dry conditions conducive to fire weather [9]. Current fire management problems (e.g., logging operations, fire suppression, water quality) in national forests may worsen due to the increase in severity and length of forest fires due to climate change. Changes in high-severity fire activity may lead to the loss of forest ecosystem resilience and the conversion of the forest structure, dominant species, life forms, or functions. In addition, increasing forest fire activity can have several adverse consequences on carbon emission, water supply, and the wildland-urban interface (WUI) [10].

The impact of air pollution or smog caused by wildfires is directly related to human health, which can cause various respiratory problems and death [11,12]. According to WHO data, air pollution has the most significant environmental impact on health, killing three million people annually [13]. Consistent evidence from many studies also indicates that wildfire smoke exposure is associated with respiratory problems such as exacerbations of asthma and chronic obstructive pulmonary disease (COPD) [14].

According to the Ministry of Environment and Forestry (KLHK) data for 2019, Indonesian wildfire spread over an area of 16,492.58 km^2 [15]. These impacts have prompted the Indonesian government to review policies and take corrective actions to improve the sustainable management of forest ecosystems [16]. In addition, the Indonesian government has committed to increasing the role of forestry in reducing GHGs as specified in the Nationally Determined Contribution program [17]. The Reducing Emissions from Deforestation and Forest Degradation in Developing Countries (REDD+) framework of the United Nations Framework Convention on Climate Change promotes policy approaches and incentive mechanisms for activities that reduce emissions from deforestation and forest degradation, conservation, sustainable forest management, and carbon stock enhancement [17].

Previous studies have conducted spatial analyses of wildfire susceptibility. Studies by Erten et al. [18] and Jaiswal et al. [19] analyzed wildfire risk zones using vegetation parameters, slope, and distance from roads and settlements. Ghorbanzadeh et al. [20] determined the readiness to deal with wildfires using vegetation, topography, climate, distance from settlements, and social factors including education level, age, facilities, and occupation

of residents. Ma et al. [21] conducted a study involving vegetation, climate, topography, and socio-economic parameters to enumerate the driving factors of wildfires. However, the disaster management approach is usually based on physical parameters. Currently available data products containing data on carbon stock [22–24] and emissions [25] can be used as additional parameters in developing susceptibility models to represent potential losses and wildfire events of the past.

The susceptibility of most regions of Indonesia to wildfires is a major challenge. In some areas, the topography is complex and accessibility is minimal. Therefore, there is a need for an in-depth study that can prioritize forest locations for wildfire mitigation. A previous study adopted an analytical approach that used physical parameters, environmental and climatic characteristics, and forest disturbances to prioritize forest restoration [26]. A spatial model for prioritizing restoration was generated based on environmental and infrastructural parameters using a multi-criteria analysis for Colombian regions [27]. A spatial prioritization model for the conservation of forest areas was designed based on Earth Observation Data, including forest biophysical parameters, forest disturbances, and burnt areas [28]. Similar research was also conducted by Tracey et al. (2018) to support wildfire management based on indicators such as threat and biodiversity using the Pareto-based multi-criteria method [29]. Raharjo and Nakoggoshi (2017) used the hierarchical analytical process (AHP) method based on forest biophysical parameters, infrastructure, threats, and the environment for conservation and rehabilitation efforts and built a spatial priority model [30]. The fire-suppression priority index was produced by Rodriguez et al. (2014) by combining potential fire behavior and suppression difficulty indexes for the prevention and suppression of wildfires [31].

The built priority models are intended individually for conservation or restoration purposes that involve partial analysis, which mostly consider only physical and social aspects. In this case, a comprehensive study involving historical and political view has not been explored to propose wildfire mitigation prioritization concept and its relation to conservation. In addition, multi-source remote sensing data products and socio-economic data have been integrated to support a comprehensive spatial analysis at the national and regional levels [32–36]. Hence, A spatial data-driven approach exposes an opportunity to analyze tropical wildfire mitigation strategy extensively from multiple aspects [37–39].

Therefore, the main objective of this study was to perform multi-dimensional analysis utilizing various types of spatial data for the prioritization of tropical wildfire mitigation. In this study, the spatial model on wildfire mitigation priorities was constructed based on susceptibility, carbon stock, and carbon emissions models. The wildfire mitigation priority area was also linked to historical data on deforestation caused by wildfires and status of land-use policies. As a novelty, disastrous, physical, social, historical, and political aspects are consolidated to support wildfire mitigation as well as conservation prioritization in Indonesia rainforests. The findings of this research contribute both for technical and administrative purposes. From a technical perspective, the outcome of this research can be used for the determination of priority areas for support through the REDD+/RAN program for wildfire mitigation. From an administrative perspective, this research can serve as a guide for the government to design spatial planning policies, especially in the forestry sector.

2. Materials and Methods
2.1. Data

A total of 20 types of data were used in this study (Table 1). Data were classified into three classes: wildfire susceptibility index (WSI), carbon stock index (CSI), and carbon emission index (CEI). Table 2 lists the three classes.

2.1.1. Climate and Atmospheric Data Products

a. MODIS Land Surface Temperature. Land surface temperature (LST) is the temperature of the earth's surface, which is a climate indicator that can be obtained from satellite

imagery. The LST data of this study were derived from MODIS TERRA satellite observations with a resolution of 1×1 km (MOD11A1.006) [42]. The annual average LST in 2019 data were obtained and processed using Google Earth Engine to analyze carbon emissions.

b. CHIRPS Rainfall Data. These data were used to determine wildfire susceptibility. Climate Hazards Group InfraRed Precipitation with Station (CHIRPS) [44] data were obtained from the USGS in the form of rainfall (precipitation) in mm/day. The monthly averages of daily data were obtained for a spatial resolution of 5.55 km.

Table 1. Data used in this study.

S. No.	Data	Source	Temporal Resolution	Spatial Resolution	Reference
1	NO$_2$	ESA	Monthly	3.5×7 km	[25]
2	SO$_2$	ESA	Monthly	3.5×7 km	[25]
3	CO	ESA	Monthly	3.5×7 km	[25]
4	Administration data	BIG	2020	Vector	[40]
5	Night light	VIIRS	Yearly	450 m	[41]
6	Land surface temperature	MODIS TERRA	Yearly	1 km	[42]
7	Population	WorldPop	Monthly and yearly	100 m	[43]
8	Precipitation	CHIRPS	Daily	5.55 km	[44]
9	Drought	KBDI	Daily	4 km	[45]
10	Wind speed	ERA5	Daily	30 km	[46]
11	Accessibility	Accessibility to Cities 2015	2015	900 m	[47]
12	Tropical forest	Primary humid tropical forest	2001	30 m	[5]
13	Global forest change	USGS	2000–2020	30 m	[48]
14	Global aboveground and belowground biomass carbon density maps	NASA	2010	300 m	[23]
15	WCMC aboveground and belowground biomass carbon density	UNEP–WCMC	2010	300 m	[24]
16	WHRC pantropical national level carbon stock dataset	Woodwell Climate Research Center	2012	500 m	[22]
17	Burned area (FireCCI51)	ESA	Monthly (2001–2019)	250 m	[49]
18	Burned area (MCD64A1)	NASA	Monthly (2000–2020)	500 m	[50]
19	Mining area	FWI	2019	Vector	[51]
20	Palm oil plantation area	FWI	2019	Vector	[51]

NO$_2$: nitrogen dioxide, SO$_2$: sulfur dioxide, CO: carbon monoxide, WCMC: World Conservation Monitoring Center, WHRC: Woodwell Climate Research Center, ESA: European Space Agency, BIG: Geospatial Information Agency of Indonesia, VIIRS: visible infrared imaging radiometer suite, MODIS: moderate resolution imaging spectroradiometer, CHIRPS: Climate Hazards Group Infrared Precipitation with Station Data, KBDI: Keetch–Byram drought index, ERA5: European Center for Medium-Range Weather Forecasts (ECMWF) reanalysis 5th generation, USGS: United States Geological Survey, NASA: National Space Agency of United States, UNEP–WCMC: United Nations Environment Program World Conservation Monitoring Center, and FWI: Forest Watch Indonesia.

Table 2. Data sharing based on data processing.

S. No.	Data	Wildfire Susceptibility Index	Carbon Stock Index	Carbon Emission Index
1	NO_2	-	-	✓
2	SO_2	-	-	✓
3	CO	-	-	✓
4	Administration data	✓	✓	✓
5	Night light	-	-	✓
6	Land surface temperature	-	-	✓
7	Population	✓	-	-
8	Precipitation	✓	-	-
9	Drought	✓	-	-
10	Wind speed	✓	-	-
11	Accessibility	✓	-	-
12	Tropical forest	✓	✓	✓
13	Global Forest change	-	✓	-
14	Global biomass carbon density maps	-	✓	-
15	WCMC biomass carbon density	-	✓	-
16	WHRC carbon stock dataset	-	✓	-

c. KBDI Drought Data. These data were used as climate parameters to determine wildfire susceptibility. The product used was the Keetch–Byram Drought Index (KBDI) [45] issued by the University of Tokyo, Japan. KBDI is computed with the land surface temperature observed from the Japanese geostationary satellite, Advanced Himawari-8 Imager (AHI) and rainfall from Global Satellite Mapping of Precipitation (GSMaP) data. The KBDI is obtained from an estimate of soil drought and it is commonly used in drought monitoring. The monthly averages of daily data were obtained for a spatial resolution of 4 km.

d. ERA-5 Wind Speed Data. Wind speed is a climate parameter that was used to determine wildfire susceptibility. Data from ERA-5, which is a climate analysis product from the European Center for Medium-Range Weather Forecasts (ECMWF) [46], containing various components were used for this purpose. The U and V components of wind speed were utilized. Monthly averages of daily data were obtained for a spatial resolution of 270 km.

e. Sentinel-5P Data. Gas emission data were obtained from Sentinel-5P Level 2 (CO, NO_2, and SO_2) [25]. These data were released by ESA in 2018 with a spatial resolution of 3.5×7.5 km and a temporal resolution of one day. Sentinel-5P data can be converted into air quality data using the differential optical absorption spectroscopy method. These data were used for time-series observations of emission patterns in the atmosphere and for correlation analysis between emissions from wildfires.

2.1.2. Forestry Data Products

a. Tropical Forest (PHTF). This product developed by the Global Land Analysis and Discovery (GLAD) team from the University of Maryland using Landsat images with a resolution of 30 m represents primary humid tropical forest (PHTF) [5]. Tropical forest areas in this product are represented by a value of 1.

b. Pantropical National Level Carbon Stock Dataset Above-ground Biomass (WHRC). This data product of the WHRC Pantropical National Level Carbon Stock Dataset [22] provides aboveground biomass density maps for tropical countries with a spatial resolution

of 500 m. These data were produced from a combination of field measurements, LiDAR observations, and MODIS imagery.

c. Global Above-ground and Below-ground Biomass Carbon Density (NASA ORLN DAAC). NASA ORLN DAAC Carbon density product [23] provides information on above- and below-ground biomass carbon density information for 2010 at a spatial resolution of 300 m. Above- and below-ground biomass carbon density maps were integrated separately using different tree cover extents and land cover maps based on decision tree rules.

d. Above-ground and Below-ground Biomass Carbon Density (WCMC). WCMC Above- and below-ground biomass carbon density data products [24] represent the storage of terrestrial carbon above and below the ground surface (C, ton per hectare) for 2010 with a spatial resolution of 300 m. Carbon stock data products as inputs were identified through datasets from previous literature on carbon biomass in terrestrial ecosystems.

e. Data (MCD64A1). The MCD64A1 Burned Area [50] is a global monthly burned area data product with a spatial resolution of 500 m that is available for 2000–2020. MCD64A1 uses a 500-m Moderate Resolution Imaging Spectroradiometer (MODIS) image plus MODIS active wildfire observations for 1 km. This data product uses an algorithm with a vegetation index (VI) that is sensitive to the burned area. A range of data product values is encoded in one data layer as the ordinal day of the calendar year in which the wildfire occurred and is denoted with a value of 1–366. A value of 0 is assigned to pixels of unburned soil, lost data, and water.

f. Burnt Area Data (FireCCI51). The MODIS burnt area pixel product version 5.1 Fire Climate Change Initiative 51 (FireCCI51) is a global monthly 250-m spatial resolution dataset containing information on burned areas [49]. This data product is based on surface reflectance in the near infrared (NIR) band from the MODIS instrument mounted on the Terra satellite and active wildfire information from the Terra and Aqua satellites. The FireCCI51 dataset includes each pixel, the estimated day of first fire detection, the confidence level of the detection, and the burnt land cover (extracted from the ESA CCI Land Cover v2.0.7 dataset).

g. Global Forest Change (GFC). GFC is a global forest data product with a spatial resolution of 30 m [48]. These data provide forest cover, where trees are defined as vegetation with a height of more than 5 m. Forest loss is defined as the disturbance of stand replacement or the change from the forest to non-forest state during 2001–2020. Forest gain is defined as the inverse of loss or the change from the non-forest to the forest state during 2000–2020.

2.1.3. Socio-Economic Data Products

a. VIIRS Night Light Data. Night light data are data on the reflection of light on the Earth's surface at night that is sourced from the Colorado School of Mines [41]. These data aim to determine the correlation between air emission and its relation to sources of human activity emissions. Night light data have a spatial resolution of 350 × 450 m and the range of these data values is 1.5 to 193,564.92 nanoW/cm^2/sr.

b. WorldPop Population Density Data. These data reflect human activity for the determination of wildfire susceptibility. The WorldPop Population Count 2019 data product was used [43]. Data released by WorldPop indicate the population per pixel with a pixel resolution of approximately 1 km.

c. Data on Accessibility to Cities (University of Oxford and JRC). These data also reflect human activity for the determination of wildfire susceptibility. The Accessibility to Cities 2015 data product developed by the Oxford Malaria Atlas project was used [47]. Data show the travel time in minutes from each pixel in an area to the nearest densely populated place with a resolution of approximately 900 m.

d. Distribution of Oil Palm and Mining areas. Data on oil-palm plantations and mining areas pertaining to Indonesia were derived from Forest Watch Indonesia (FWI) for 2019 [51]. Oil palm data are in the form of vectors indicating legal cultivation rights obtained in the name of companies. Mining data is in the form of vector data on areas indicating mining

permits. These data also contain names of companies, number of legal decrees, type of permit, mining stage (exploration or production operation), commodity, and status.

2.2. Methodology

This study comprehensively covered five aspects in the analysis, including wildfire susceptibility, carbon stock, carbon emissions, deforestation hotspots, and land use policy. Figure 1 illustrates the framework of this study.
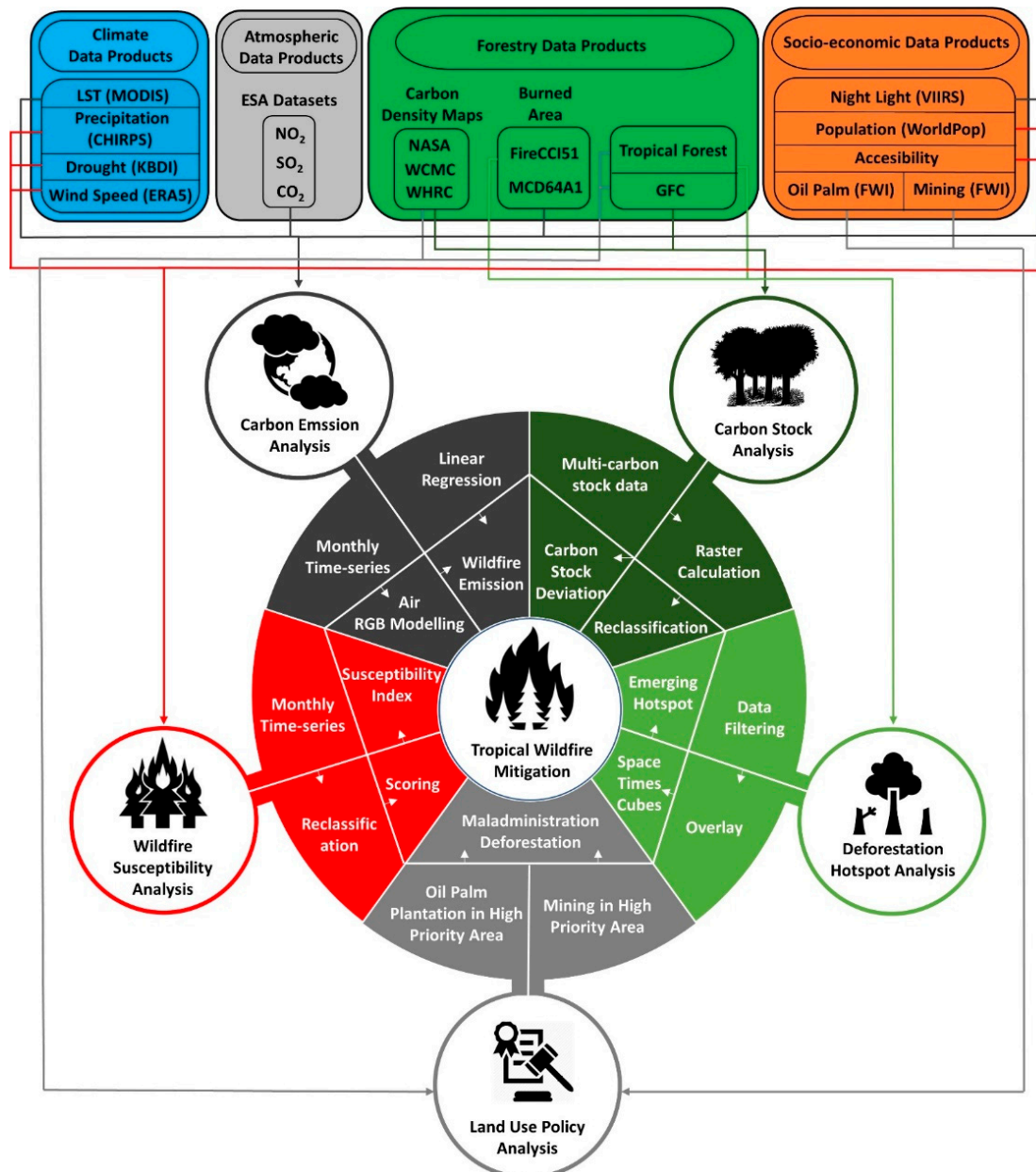

Figure 1. Flowchart of data processing. LST: land surface temperature, NO_2: nitrogen dioxide, SO_2: sulfur dioxide, CO: carbon monoxide, WCMC: World Conservation Monitoring Centre, WHRC: Woodwell Climate Research Center, ESA: European Space Agency, VIIRS: Visible Infrared Imaging Radiometer Suite, MODIS: Moderate Resolution Imaging Spectroradiometer, FireCCI51: Fire Climate Change Initiative 51, MCD64A1: MODIS burned area data, CHIRPS: climate hazards group infrared precipitation with station data, KBDI: Keetch–Byram drought index, ERA5: ECMWF reanalysis 5th generation, and FWI: forest watch Indonesia.

2.2.1. Wildfire Susceptibility Index

The wildfire susceptibility index for each pixel was determined using five parameters, that is, drought, wind speed, rainfall, population, and accessibility. The next step was to score each class through reclassification with a range of 1 to 5. The five parameters were then summed to obtain the wildfire susceptibility index using Equation (1):

$$WSI = Ds + Rs + Ws + Ps + As \tag{1}$$

where, WSI is the wildfire susceptibility index and Ds, Rs, Ws, Ps, and As are the drought, rainfall, wind speed, population, and accessibility scores, respectively. The wildfire susceptibility index was classified into five susceptibility classes based on quantile classifiers [45].

2.2.2. Carbon Stock Index

Carbon stock data includes above- and below-ground biomass from WHRC above-ground, WCMC above-ground, and below-ground carbon stock data, and global above-ground and below-ground biomass carbon density maps. In this case, the above-ground biomass was exploited to represent the carbon stock loss due to crown fires and surface fires. While, the below-ground biomass was used to represent sub-surface fires which frequently occur in Indonesian peatlands region. The initial step was to obtain a uniform spatial resolution using a technique that equates the resolution of data to 500 m. The mean value was then calculated to obtain *CSI* and standard deviation to determine the variation in carbon stock data.

$$CSI = \frac{\text{WCMC}_{A\&B} + \text{Global}_A + \text{Global}_B + \text{WHRC}_A}{4} \tag{2}$$

$\text{WCMC}_{A\&B}$ = Above-ground and below-ground biomass.
Global_A = Above-ground biomass.
Global_B = Below-ground biomass.
WHRC_A = Above-ground biomass.

$$STD = \sqrt{\frac{\sum_{i=1}^{n}\left(Xi - \overline{X}\right)^2}{n-1}}$$

$$STD = \sqrt{\frac{\left(Xwcmc_{agb} - \overline{X}\right)^2 + \left(Xglobal_{agb} - \overline{X}\right)^2 + \left(Xglobal_{bgb} - \overline{X}\right)^2 + \left(Xwhrc_{agb} - \overline{X}\right)^2}{n-1}} \tag{3}$$

STD = Standard deviation.
X_i = Carbon stock data.
$\overline{X}$ = Mean carbon stock.
n = Number of carbon stock data.

2.2.3. Carbon Emission Index

Sentinel-5P data were processed to create a monthly model of gas emissions (CO, NO_2, and SO_2) in Indonesia for 2019. The initial stage involved layer stacking with the red band 'R' as CO gas, 'G' as NO_2 gas, and the blue band, 'B' as SO_2 gas, to form the Air–RGB model. The Air–RGB model was adapted and modified based on the research of Misra and Takeuchi (2017) [52], who evaluated air quality in urban areas by observing aerosol optical depth (AOD) and the Angstrom exponent. Gas emission calculations were combined with the Air–RGB model based on latitude and longitude to determine the trend of air emissions in each area. Furthermore, data on the Earth's surface temperature, night lights, and population were correlated with each gas emission. In addition, data for each air emission were classified into five classes to obtain the CEI value.

2.2.4. Wildfire Priority Index (WPI)

WSI, CSI, and CEI with different spatial data resolutions were equalized to a 1-km spatial resolution to produce a priority index model for wildfire mitigation. WSI determines forest areas that are prone to burning. CSI determines large forest areas and areas with high carbon sequestration potential. CEI indicates air emissions or pollutant sources in the burned area. The method that integrates these indices uses quantile classification to distribute a group of attribute values into classes containing the same amount of data [53]. The three indices are integrated based on Equation (4) to produce a priority model of wildfire mitigation in Indonesia, which is classified into three priority classes of high, medium, and low.

$$WPI = WSI + CSI + CEI \tag{4}$$

2.2.5. Emerging Hostpot

Hotspot analysis aims to identify trends in the clustering point density in the burned area. This study used spatial analysis based on the location and time of events collected together into a bin referred to as the emerging hotspot analysis [54]. Emerging hotspots evaluate spatiotemporal patterns using a combination of two statistical measures, namely Getis-Ord Gi (Equation (2)) and the Mann–Kendall trend test using GFC data, that is, MCD64A1 and FireCCI51 for 2010–2019. Each bin had a Z score and a p value. The larger the positive Z score, the more intense the grouping that forms the hotspot negative Z score. The lower the Z score and negative score, the lower the group that includes the coldspot [55].

$$G_i{}^* = \frac{\sum\limits_{j=1}^{n} wi,jxj - \overline{X}\sum\limits_{j=1}^{n} wi,j}{S\sqrt{\dfrac{\left[n\sum\limits_{j=1}^{n} \cdot \ wi^2,j - \left(\sum\limits_{j=1}^{n}\cdot \ wi,j\right)^2\right]}{n-1}}} \tag{5}$$

$$\overline{X} = \frac{\sum\limits_{j=1}^{n} xj}{n} \tag{6}$$

$$s = \sqrt{\frac{\sum\limits_{j=1}^{n} xj2}{n} - \left(\overline{x}\right)2} \tag{7}$$

xj is the attribute value for feature j, wi,j is the spatial weight between features i and j, and n is the number of features. Furthermore, the trends of hotspots and coldspots were evaluated using the Mann–Kendall trend test to identify categories of hotspots and coldspots. The emerging hotspot was applied for annual deforestation collected from GFW during 2010–2020. The result was compared to the wildfire priority model as a consistency assessment approach was used in this study.

3. Results

3.1. Wildfire Susceptibility Model

Wildfire susceptibility was classified into very-low, low, medium, high, and very-high, as shown in Figure 2. From January to June, very-low-and low-susceptibility classes dominated the territory of Indonesia. The emergence of areas with high to very-high susceptibility classes began in July and peaked in September. Areas with high and very-high classes experienced a decrease in area during October. Very-low susceptibility classes dominated Indonesian forests during November and December, following the seasonal cycle in the tropics. Figure 3 shows an in-depth analysis of the patterns of area per class per month and the overall average for one year. Based on the monthly location for each class, the total of the very-low class peaked in January (676,152.27 km^2), low class in

June (273,126.6 km^2), medium class in September (294,217.1 km^2), high class in August (168,668.1 km^2), and very-high class in August (23,429.88 km^2). Based on these results, the potential for wildfire susceptibility in Indonesia's tropical forests in the third quarter of 2019 is a matter of concern.
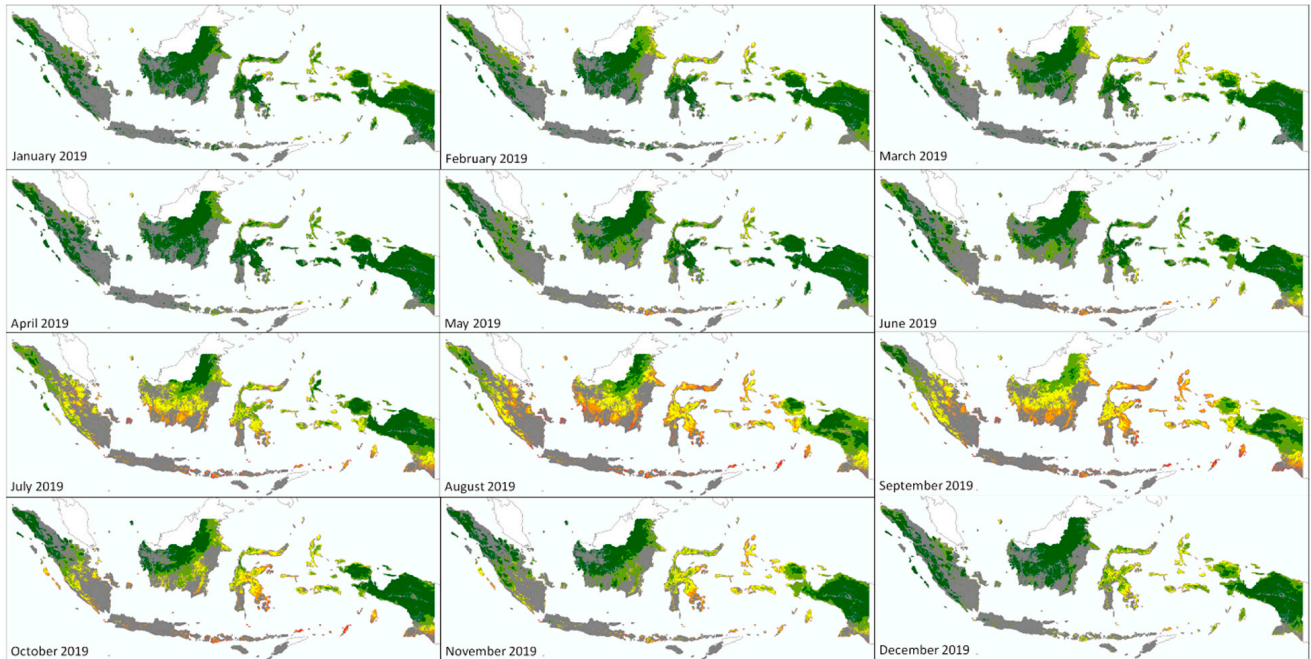

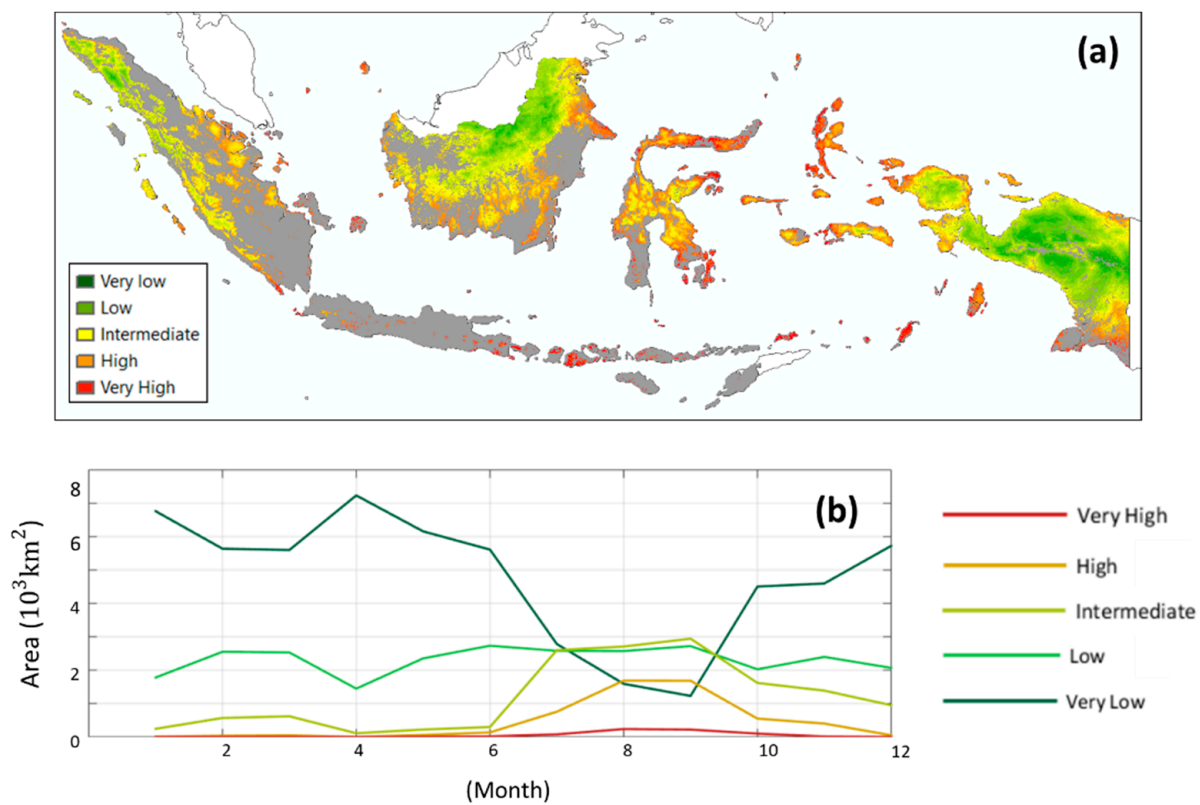**Figure 2.** Wildfire susceptibility classes in Indonesia for each month of 2019.

Figure 3. (**a**) Wildfire susceptibility classes in Indonesia in 2019 and (**b**) time-series of monthly area patterns for each susceptibility class.

3.2. Carbon Emission Model

According to Pribadi and Kurata (2017) [56], gas emissions from forest fires are dominated by CO gas. This finding is also relevant based on the correlations observed between population, night light, and Environmental, Social, and Governance (ESG) represented by LST with CO gas emissions, as shown in Figure 4. In this case, population and night light represent human activities, while ESG (LST) represents wildfires. The results of the correlation analyses showed that LST and CO have a higher positive correlation than that of night light and population, indicating that an increase in ESG corresponds to an increase in CO gas emissions. Analysis of the Air–RGB decomposition model of air quality parameters, including CO, SO_2, and NO_2, was used to understand their distribution.
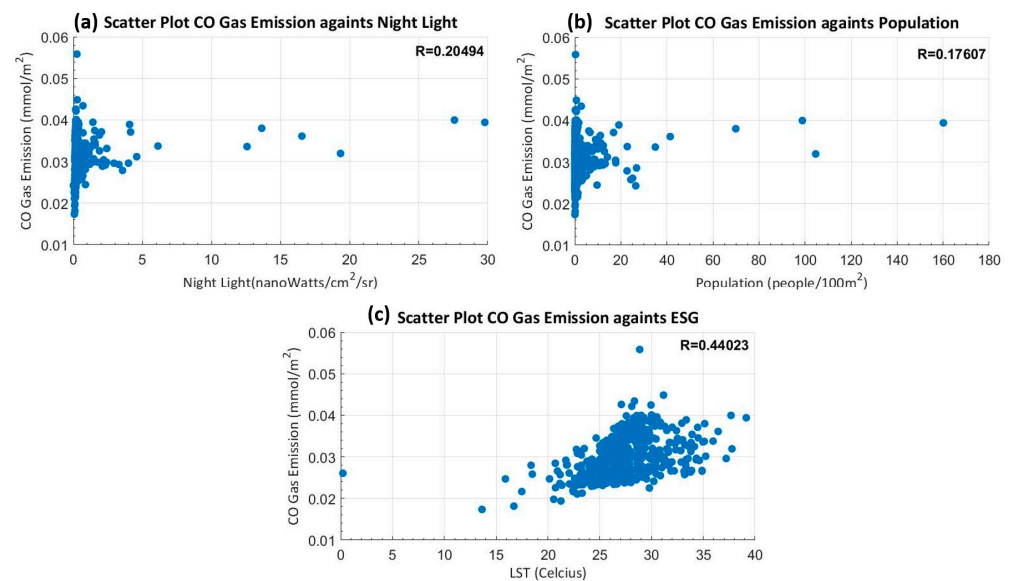
Figure 4. Correlations of air quality with (**a**) night light, (**b**) population, and (**c**) Environmental, Social and Governance (ESG).

Figure 5 shows that the pollutants in Sumatra were dominated by NO_2 and CO gases. This phenomenon indicates that human activities in urban areas are directly proportional to the population. According to Badan Pusat Statistik, Indonesia data (2020), Sumatra Island has a middle-class population density of 72–267 persons/km^2 [57]. In addition, high CO gas also indicates wildfires. According to KLHK data (2020), the area engulfed by forest fires in Sumatra in 2019 reached 5357.88 km^2, with 3064.36 km^2 occurring on mineral-bearing lands and 2293.51 km^2 on peatlands [15]. Kalimantan was dominated by CO gas, which indicates the existence of wildfire. KLHK data records that the wildfire area in Kalimantan in 2019 reached 6845.99 km^2 with 4226.50 km^2 on mineral-bearing lands and 2619.50 km^2 on peatlands [15].

Monthly time-series analysis for 2019 showed that the highest CO levels occurred in September in Sumatra and Kalimantan (Figure 6). This phenomenon was confirmed by KLHK data obtained through TERRA/AQUA by Lembaga Penerbangan dan Antariksa Nasional (LAPAN) [58]. The highest number of hotspots (16,178) occurred in September. KLHK data showed that in Sumatra hotspots occurred in the provinces of Jambi, Riau, South Sumatra, and Lampung with areas of 565.93, 905.50, 3367.98, and 355.46 km^2, respectively [15]. LAPAN data showed 2705, 1055, 1507, and 100 hotspots, respectively in these areas [59]. In Kalimantan, wildfire hotspots occurred in the region between 109°–117° longitude and 3°–5° latitude, mainly in the West, South, Central, and East Kalimantan provinces with consecutive wildfire areas in 2019 with areas of 1519.19, 1378.48, 3177.49, and 685.24 km^2, respectively, according to KLHK data (2020) [15], and the number of hotspots-derived LAPAN data (2020) were 2656, 548, 5574, and 749, respectively.
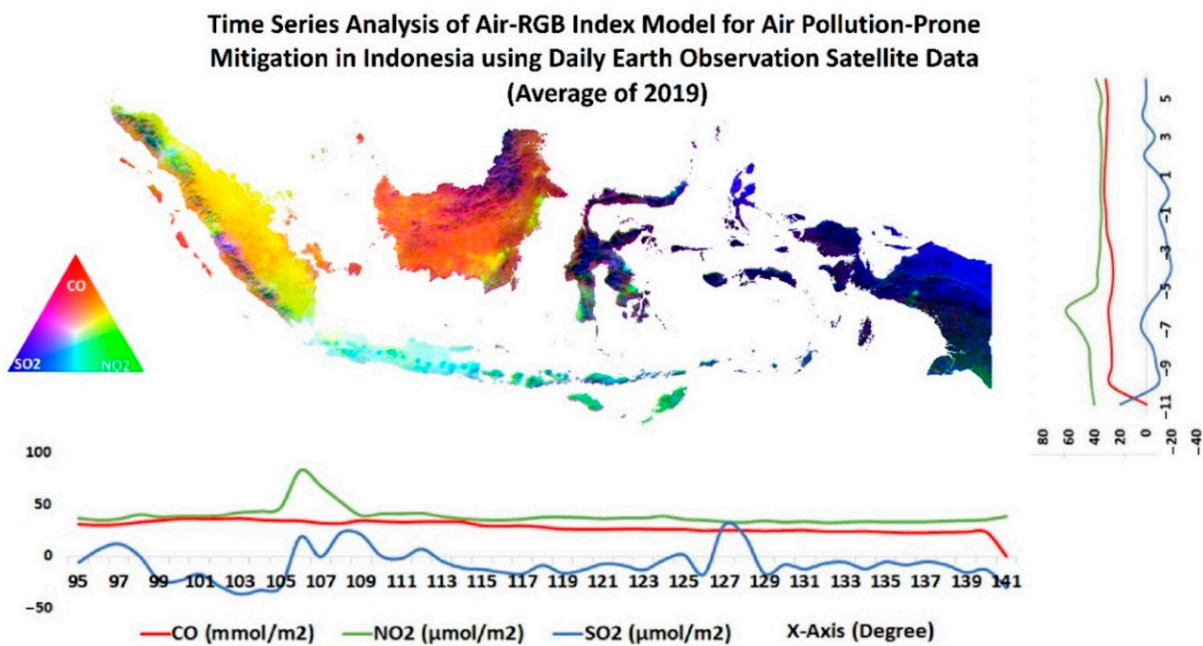
Figure 5. Times series analysis of Air–RGB model indicating air quality of Indonesia using monthly averages of daily Earth Observation Satellite data for the mitigation of wildfire (average 2019).
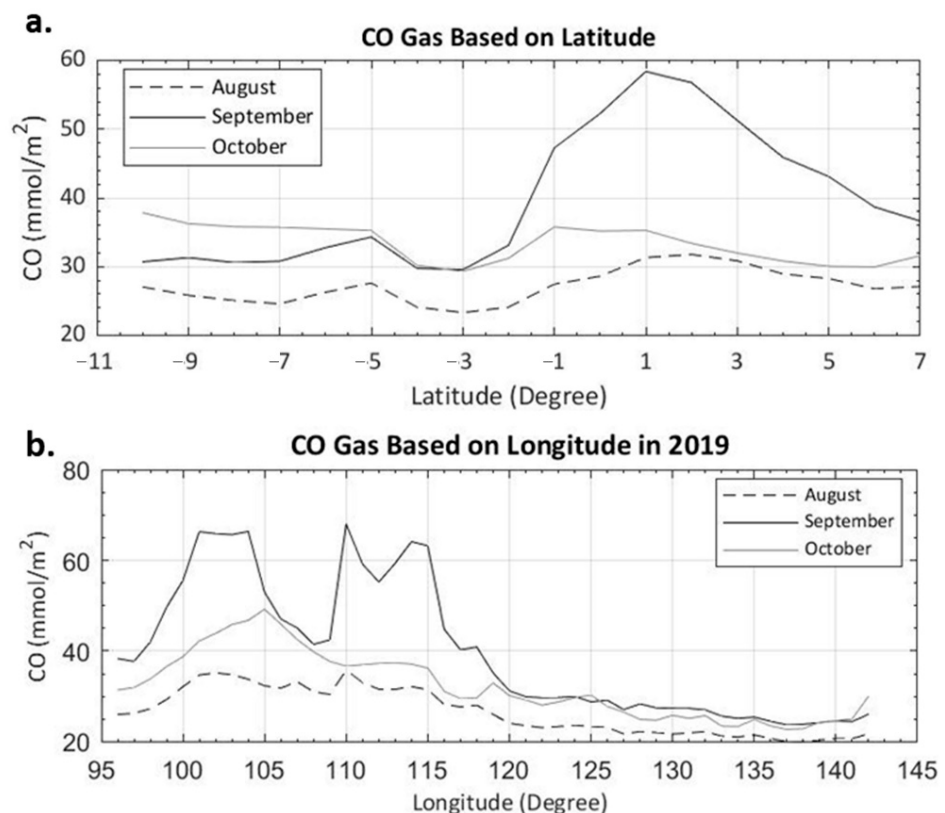

Figure 6. CO gas time-series data based on (**a**) latitude and (**b**) longitude for 2019.

3.3. Carbon Stock Model

The highest mean carbon stock obtained in this study was 996,951 tons per ha, while the highest standard deviation was 1135.41 tons, indicating that carbon stock data vary widely (Figure 7a). The Papua region has a high standard deviation as indicated by the variations in the distribution of high concentration hotspots (in red). Variations in standard

deviation show that biomass varies, indicating that it is challenging to identify individual forest carbon stock for each area. Therefore, the three biomass products were integrated by calculating the mean of the aboveground and belowground carbon stock data (Figure 7a). The carbon stock model was then classified into five classes (Figure 7b).
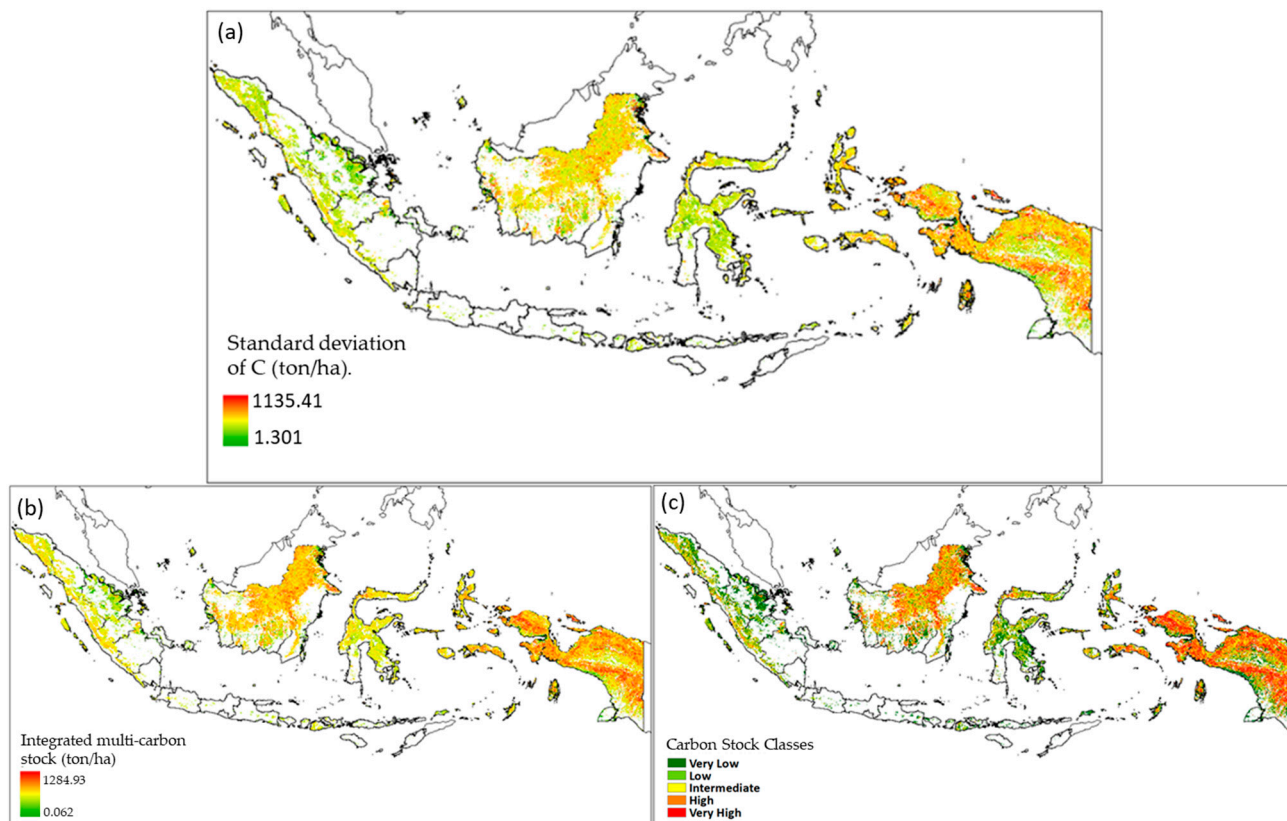

Figure 7. (**a**) Standard deviation of C content derived from the multi-carbon stock model. (**b**) Integrated multi-carbon stock, and (**c**) carbon stock classes.

3.4. Priority Model for Wildfire Mitigation

The priority model for wildfire mitigation in Indonesia was generated by integrating susceptibility, carbon stock, and carbon emission models (Figure 8). In Kalimantan, Sumatra, and North Maluku, the number of priority areas was high. In addition, these areas are also dominated by forest areas with high carbon stocks. On the other hand, Papua and Sulawesi have low priority because they have a low level of wildfire susceptibility even though they have high carbon stocks. Java and Bali have small areas of forests and low carbon stocks and therefore, the wildfire priority areas in these regions were relatively low. Figure 9 shows the ten provinces with the highest priority for wildfire mitigation in Indonesia. These provinces are located in Kalimantan, Sumatra, and North Maluku. South Kalimantan had the highest high-priority area of 6582 km^2, a medium-priority area of 9173 km^2, and a low-priority area of 54 km^2. However, based on the size of the highest-priority area, Central Kalimantan had the most extensive high-and medium-priority areas at 37,357 km^2 and 64,229 km^2, respectively. In Riau, the priority areas were dominated by medium and high classes, indicating that the forest in the area needs special attention. North Kalimantan was dominated by low-priority wildfire areas owing to its low susceptibility index and CO gas emissions. In terms of forest land management, North Kalimantan is a primary forest area in which mining or oil-palm plantation permits have not been issued. High-priority regions, such as the Northeast, Central, and South Kalimatan, are forest areas whose concessions are owned by mining companies or oil-palm plantations.
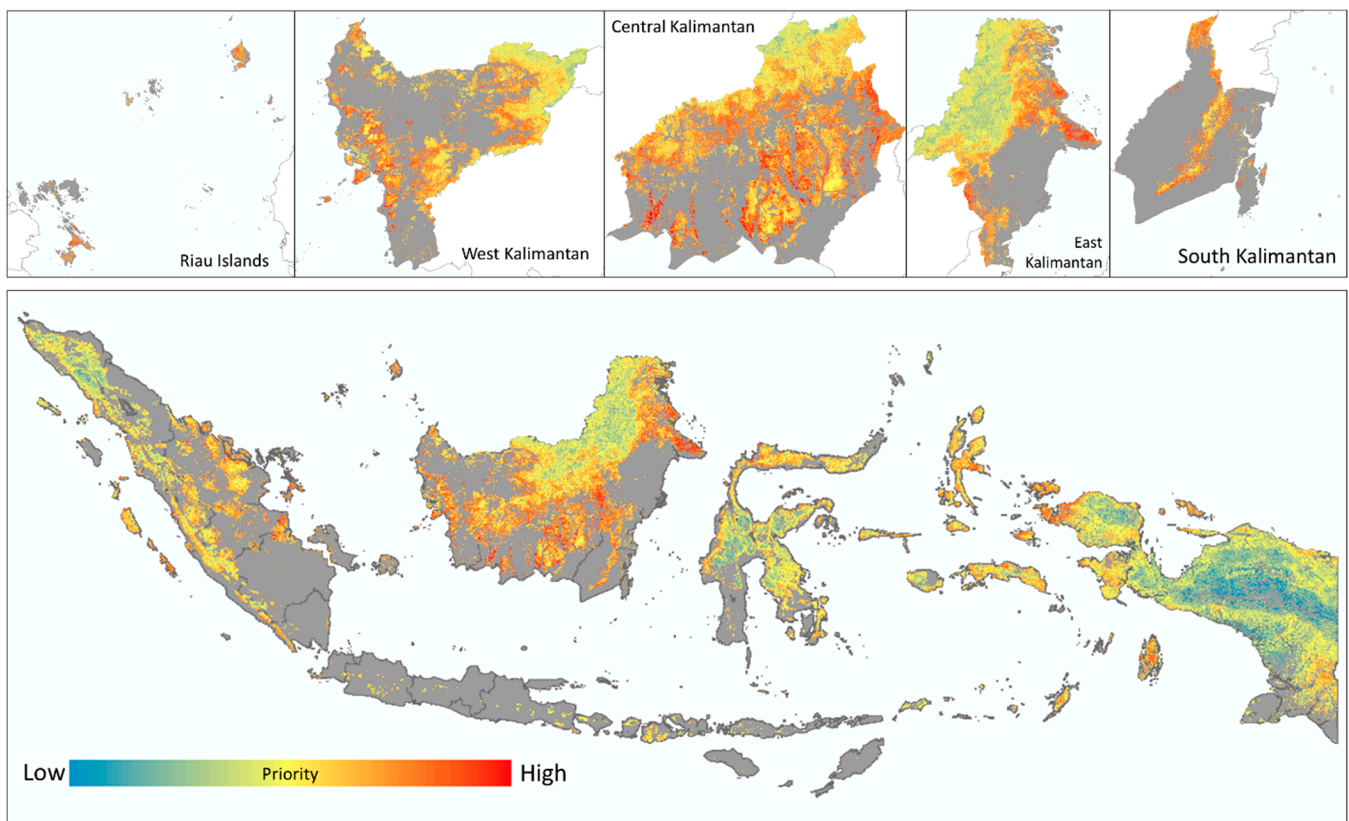
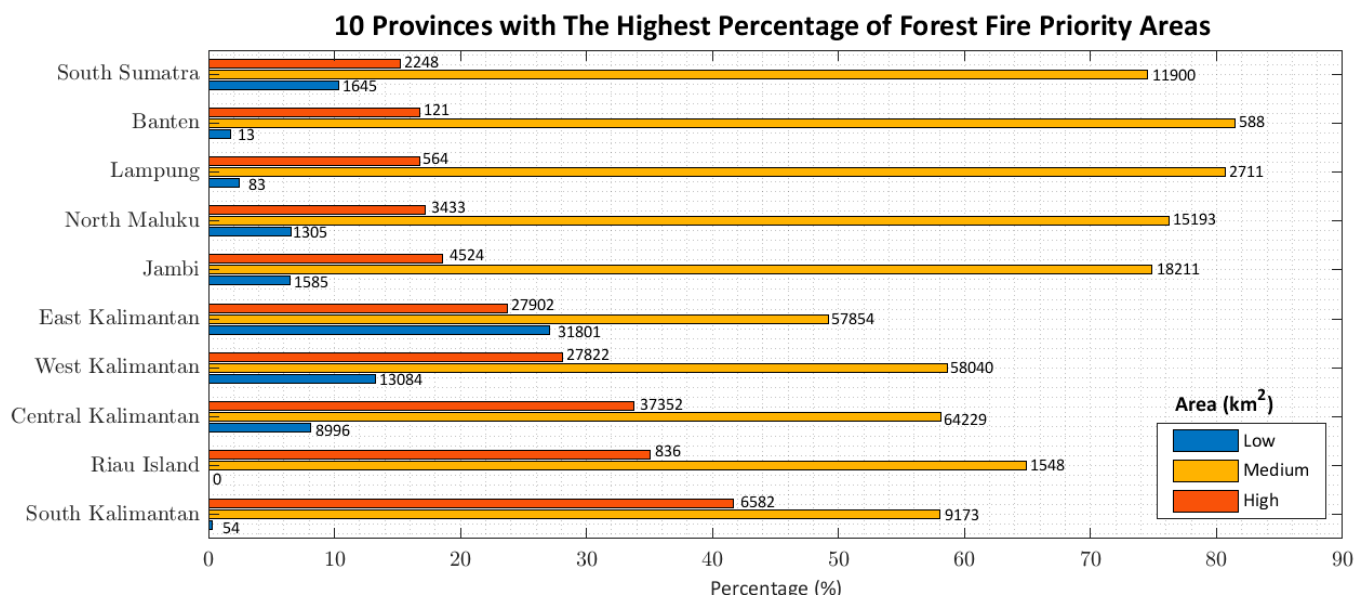**Figure 8.** Priority areas for wildfire mitigation in Indonesia.

Figure 9. Top ten provinces based on percentage of priority areas for wildfire mitigation.

4. Discussion

4.1. Emerging Hotspots of Deforestation

Emerging hotspot analysis for 2010–2019 outlined the wildfire pattern in Indonesia. Figure 10 shows the eight classes of patterns of wildfire in Indonesia as follows: new, oscillating, consecutive, and sporadic hotspots and oscillating, persistent, sporadic, and intensifying coldspots. Figure 10 is visualized based on a 25 × 25-km grid, while Figure 10a–c is visualized in the actual data resolution of 1 km.
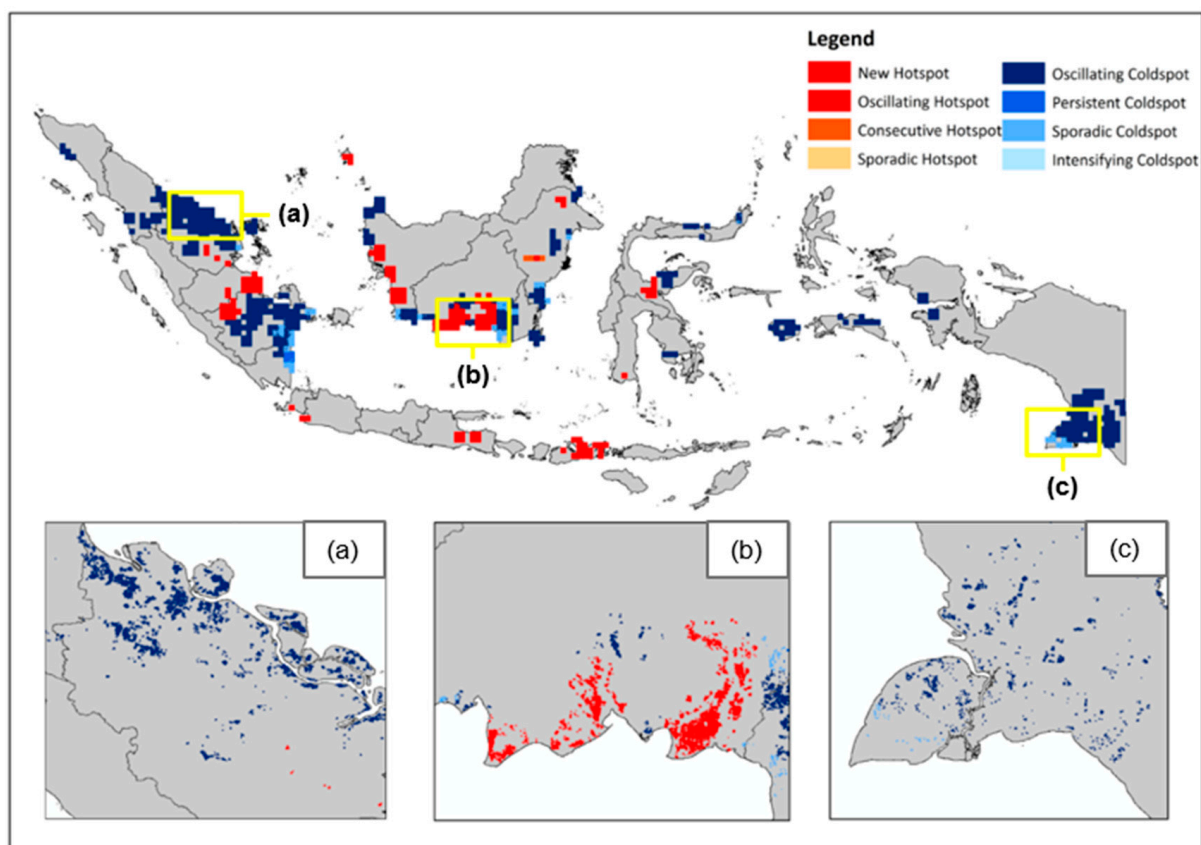
Figure 10. Emerging wildfire hotspots of Indonesia using a 25 × 25-km grid; detailed visualization using 1 × 1-km grids for the areas (**a**) Riau Province, (**b**) Central Kalimantan Province, and (**c**) Merauke Regency.

Figure 11 shows that the trends of forest fires in Indonesia are dominated by oscillating coldspot and oscillating and new hotspots. New hotspots occupy 7.009% of the area and represent statistically significant hotspot locations only during 2018 and/or 2019, i.e., during the last time step of the time series with high wildfire incidence (clustered). Oscillating hotspots occupy 19.422%, which are locations that have become statistically significant during less than 9 out of the considered 10 years (<90%) with a high incidence of wildfires (clustered). In addition, statistically significant coldspots that occurred during the previous time step have become consecutive hotspots occupying 0.061% of the area, i.e., these are locations with one statistically substantial hotspot path without interruption in the last time-step interval with a high wildfire incidence (clustered). Sporadic hotspots occupy 0.004% of the area, wherein wildfires occur randomly (unevenly) but frequently from year to year. Less than 9 out of 10 years (<90%) have become statistically significant hotspots with a high wildfire incidence (clustered). Oscillating coldspots occupy 66.115% of the area and represent locations that were statistically significant coldspots for less than 9 out of 10 years (<90%) with occurrences of dispersed wildfires. Additionally, these locations have a history of being statistically significant hotspots during the previous time step. Persistent coldspots occupy 0.249% of the area, i.e., locations that have been statistically significant coldspots for 9 out of 10 years (90%), with no visible trend showing an increase or decrease in clustering intensity over time with the occurrence of dispersed wildfire events. Sporadic coldspots occupying 7.131% of area representing locations of wildfires that occurred randomly (unevenly) but frequently from year to year. Less than 9 out of 10 years (<90%) were statistically significant cold points with dispersed wildfires. Intensifying coldspots occupy 0.009% of the area representing statistically substantial

coldspot locations for 10 years. In addition, the intensity of the high number of clustering at each time step increased with dispersed wildfire events.
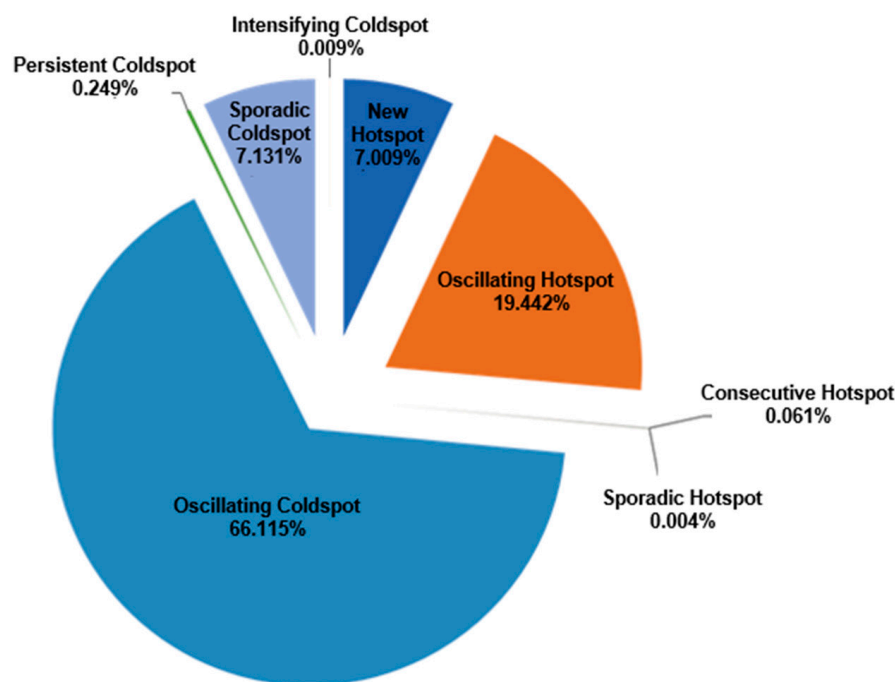

Figure 11. Pie chart of emerging hotspots.

Emerging hotspots of deforestation caused by forest fires were integrated with those of handling forest fires to prioritize wildfire mitigation (Figure 12). Hotspot categories must be prioritized for wildfire mitigation because wildfires can be high or clustered in a location. Figure 13 shows the percentage and area of wildfire priority in the hotspot area. The oscillating hotspot category had a high priority and occupied an area of 19.422%. High priority areas occupied 2.121% and encompassed an area of 159 km^2, and medium priority areas occupied 323 km^2. The new hotspot category occupied 7.009%, of which 117 km^2 or 1.189% was of high and 131 km^2 was of medium-priority levels. The priority areas in the hotspot category were Riau, Jambi, West Kalimantan, and Central Kalimantan (Figure 13).

Figure 14 shows a prioritized coldspot category in wildfire mitigation. The coldspot category has a dispersed wildfire occurrence. The coldspot category had a higher extent than the hotspot category, and therefore, it must be prioritized for wildfire mitigation. Figure 15 shows the percentages and areas of priority for wildfires in the coldspot category. Oscillating coldspots occupy the highest percentage and area of priority compared with hotspots, with a percentage of 66.12%. High-priority oscillating coldspots occupied 15.49%, amounting to 637 km^2 and a medium-priorty area of 2924 km^2. The prioritized areas in the coldspot category were Riau, South Sumatra, West Kalimantan, Central Kalimantan, and Merauke. Table 3 shows the total area of emerging hotspots and the areas of emerging hotspots in priority areas. The highest area of emerging hotspots was in the oscillating coldspot category, with an area of 15,121 km^2. The emerging hotspots located in priority areas amounted to 3647 km^2 (24.119%).
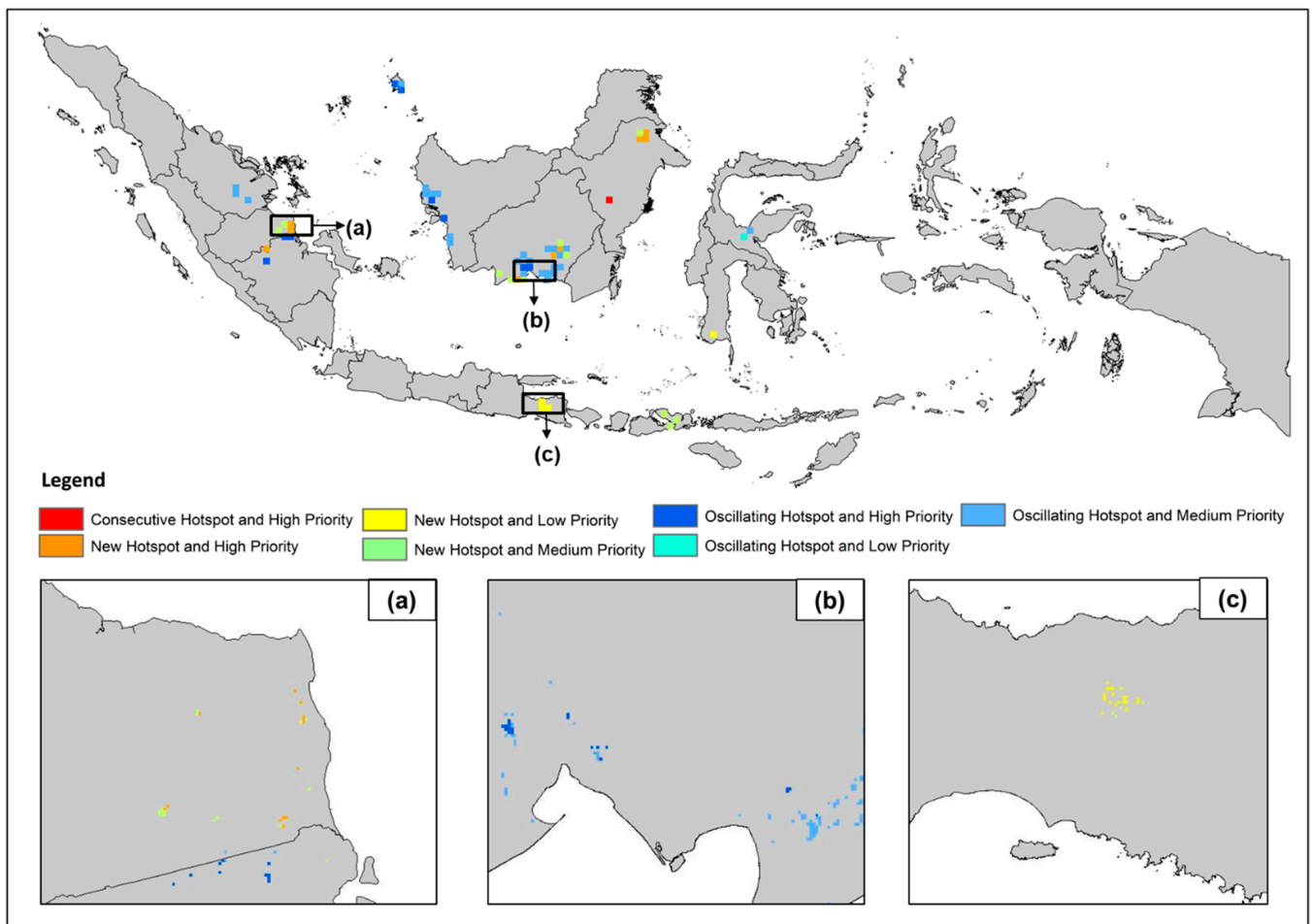
Figure 12. Prioritization for wildfire mitigation in hotspot areas using a 25 × 25-km grid. Detailed visualization using 1 × 1-km grids for the areas (**a**) Jambi Province, (**b**) Central Kalimantan Province, and (**c**) East Java Province.
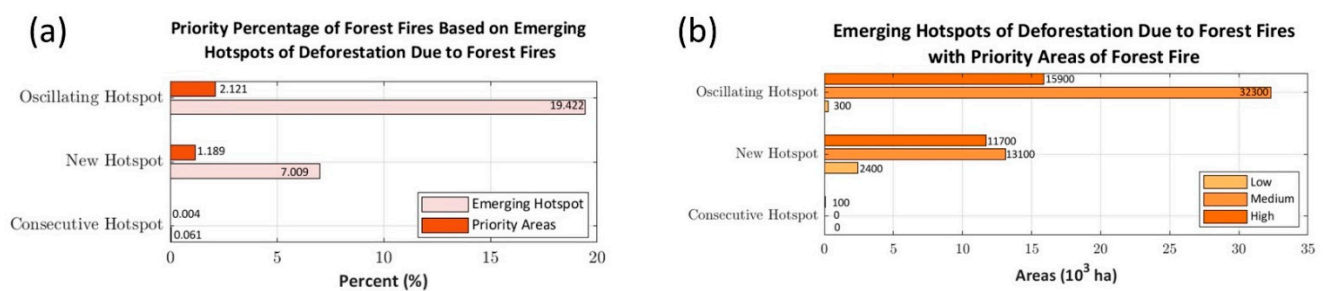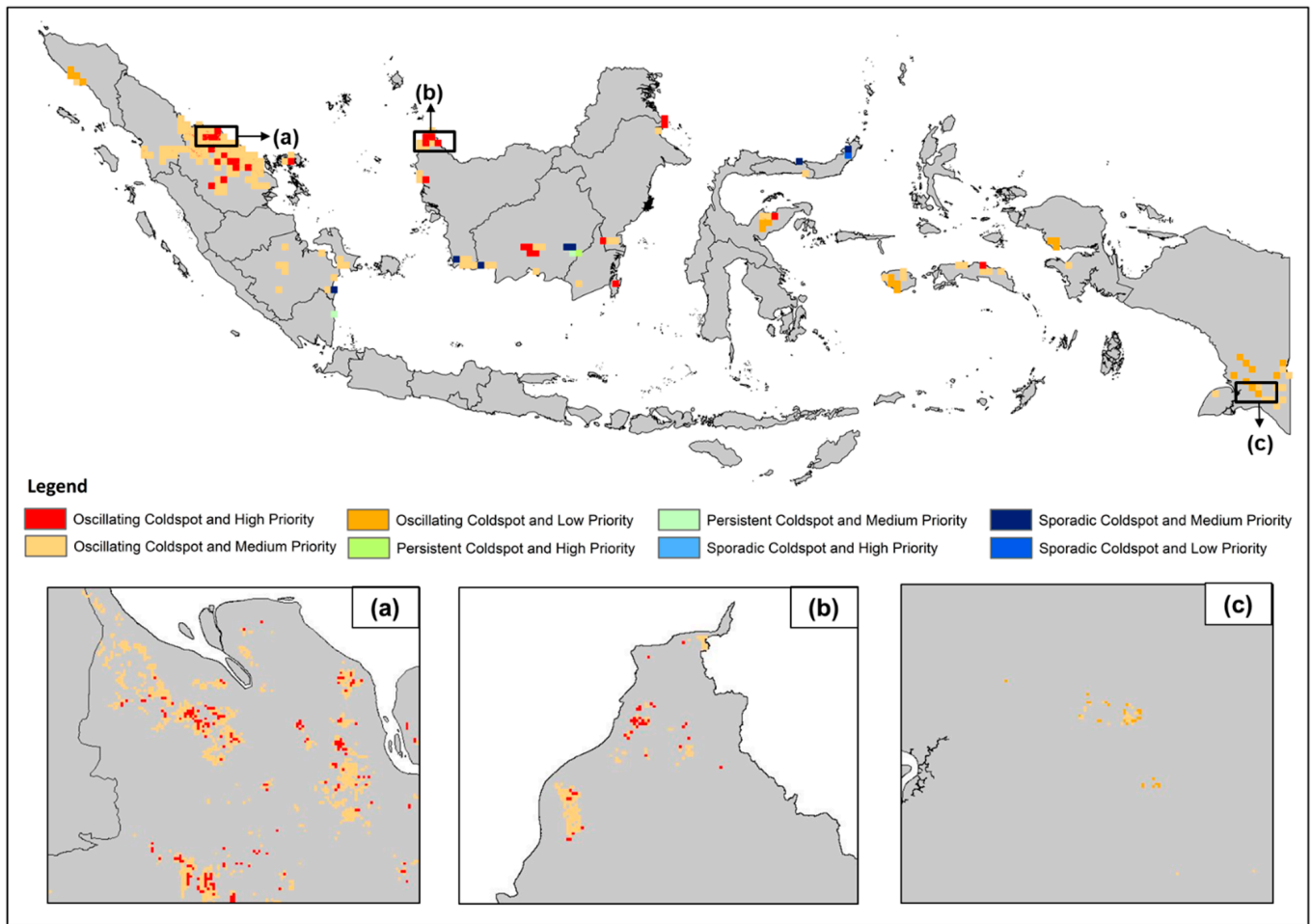

Figure 13. Priority areas for handling forest fires in emerging hotspots in the hotspot category in terms of (**a**) Percentage (%) and (**b**) Area.

Figure 14. Prioritization for wildfire mitigation in coldspot areas using a 25 × 25-km grid. Detailed visualization using 1 × 1-km grids for the areas (**a**) Riau Province, (**b**) West Kalimantan Province, and (**c**) Papua Province.

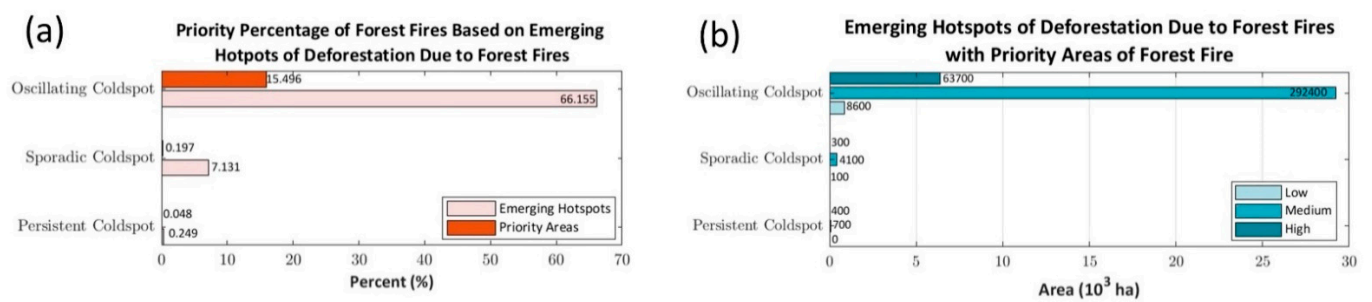**Figure 15.** Priority areas for wildfire mitigation in emerging hotspots in the coldspot category in terms of (**a**) percentage and (**b**) area.

Table 3. Total emerging hotspot area and emerging hotspot areas in the priority area.

Category	Emerging Hotspot (km²)	Emerging Hotspot in Priority Area (km²)	Percentage
New Hotspot	1603	272	16.968%
Oscillating Hotspot	4442	485	10.919%
Consecutive Hotspot	14	1	7.143%
Oscillating Coldspot	15,121	3647	24.119%
Persistent Coldspot	57	11	19.298%
Sporadic Coldspot	1631	45	2.759%

4.2. Policy Intervention

The wildfire priority area model was overlaid with mining areas and oil-palm plantations to evaluate the efficacy of government implemented forest management policies (Figure 16). Accordingly, 59,238 km^2 of forest was allocated for oil-palm plantation and 57,830 km^2 was allocated for mining areas. These amounts account for approximately 10% of the forest cover in Indonesia.
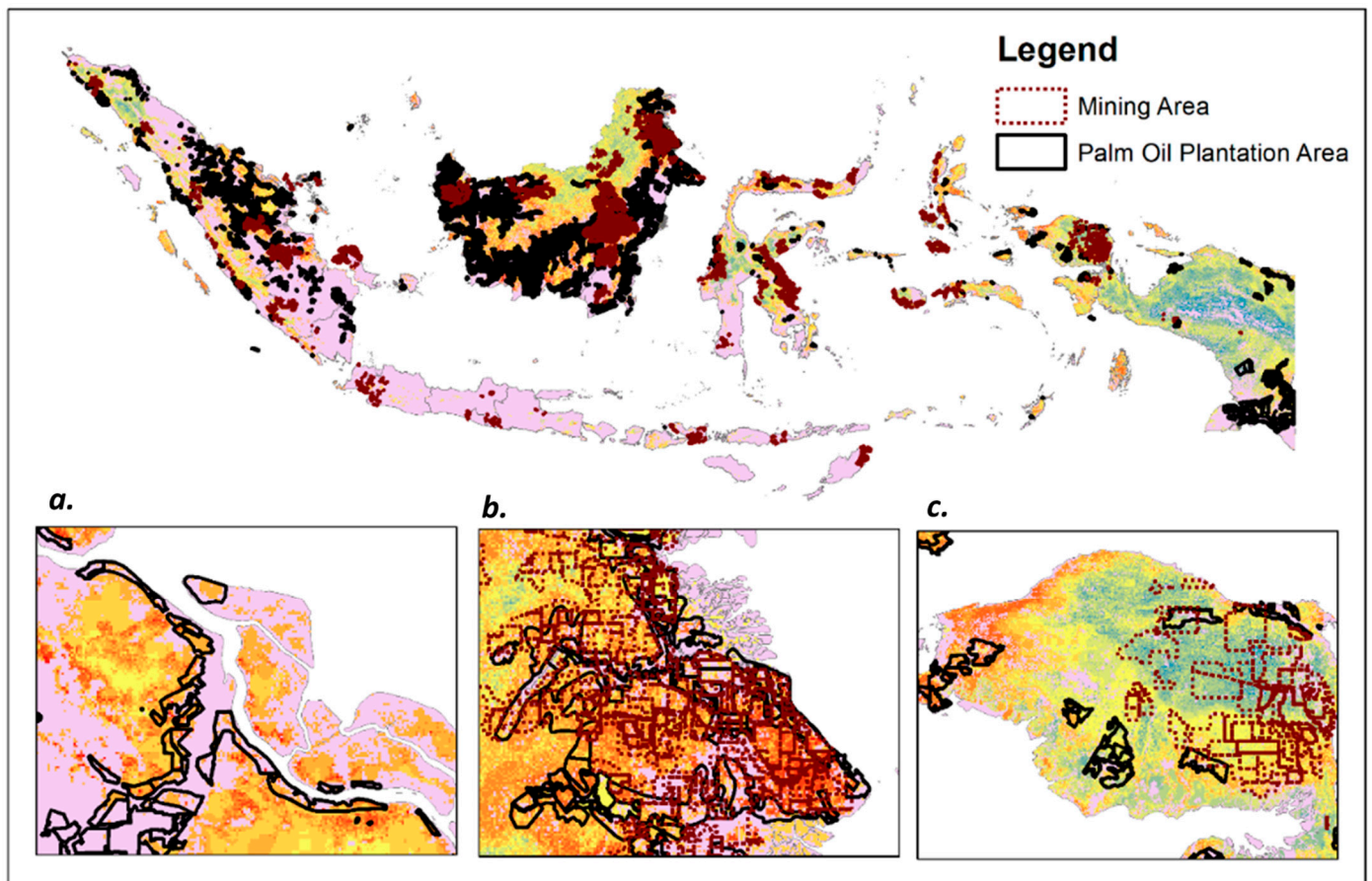

Figure 16. Wildfire mitigation in oil-palm plantation and mining areas (**a**) Riau Province, (**b**) North Kalimantan Province, and (**c**) West Papua Province.

Figure 17 shows ten provinces with the highest wildfire mitigation priority areas in oil-palm plantation areas. Central Kalimantan had the most significant medium- and high-priority wildfire mitigation priority areas in oil-palm plantation areas. This phenomenon indicates maladministration in permitting oil-palm plantations in forest areas. The higher the priority for wildfire mitigation, the more forest must be maintained. Likewise, with other provinces on the island of Kalimantan, the results of the Air–RGB model showed that air quality was dominated by the concentration of CO. If the forest cover decreases, air quality in the area can worsen because the forest can release CO_2. In contrast to the Papua Province, although oil-palm plantations in forest areas are among the largest, the priority for wildfire mitigation was dominated by low- and medium-priority classes, indicating no concern. However, monitoring must be conducted to prevent ineffective land use policies in Sumatra and Kalimantan. Moreover, the CSI model suggested that the Papua Province has the highest carbon stock. Therefore, although wildfire mitigation priority tends to be low, it does not mean that deforestation is low because of the expansion of oil-palm plantations or mining.
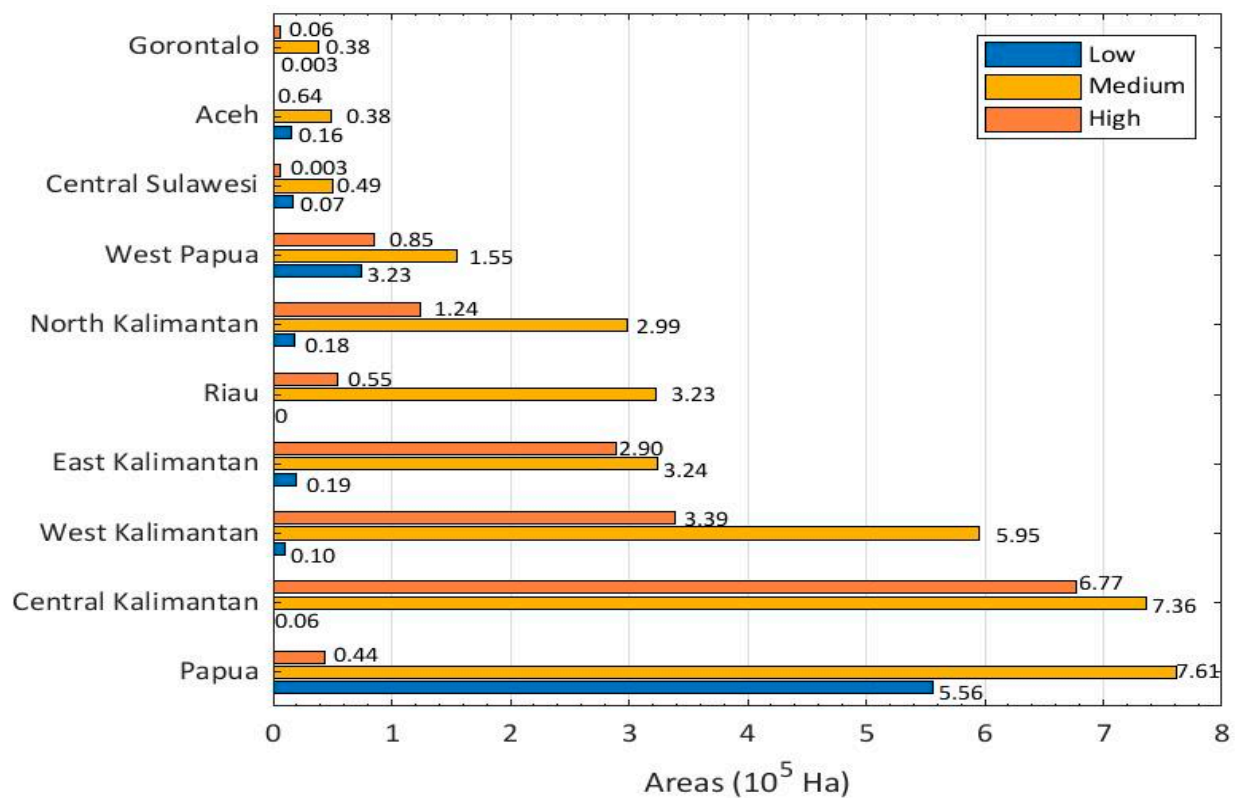
Figure 17. Top ten provinces based on priority areas for wildfire mitigation in oil-palm plantation areas.

Figure 18 shows the top ten provinces in terms of priority for wildfire mitigation in mining areas. Areas in Kalimantan dominantly displayed high priority. This phenomenon shows the existence of maladministration because this province does not permit large-scale forest clearing for oil-palm plantations and mining. West Papua Province ranked second, which indicates the most significant priority for wildfire mitigation in mining areas. The emergence of Maluku and North Maluku Provinces in the ten highest priority provinces is interesting because their sizes are relatively small compared with the other provinces, indicating that forest management in eastern Indonesia is still weak and it faces a threat because of large-scale deforestation. Central Sulawesi also needs special supervision because it appears in the top ten priority provinces for wildfire mitigation, both in terms of oil-palm plantations and mining. Riau Province appears in this list because of the large extent of palm oil plantations in it; however, it is not the top province in terms of wildfire mitigation because most of the forests in the province have already been been deforested. An extension of the moratorium on oil-palm plantation permits can delay their addition of in forest areas and reduce deforestation. During the moratorium, policymakers and permit owners in forest areas must evaluate the progress of forest management and design programs to mitigate wildfires. Other aspects, such as the one-map policy, can also be optimized. All forestry data must have one standard and one database, including company concessions in non-overlapping forest areas leading to refinement of policies.
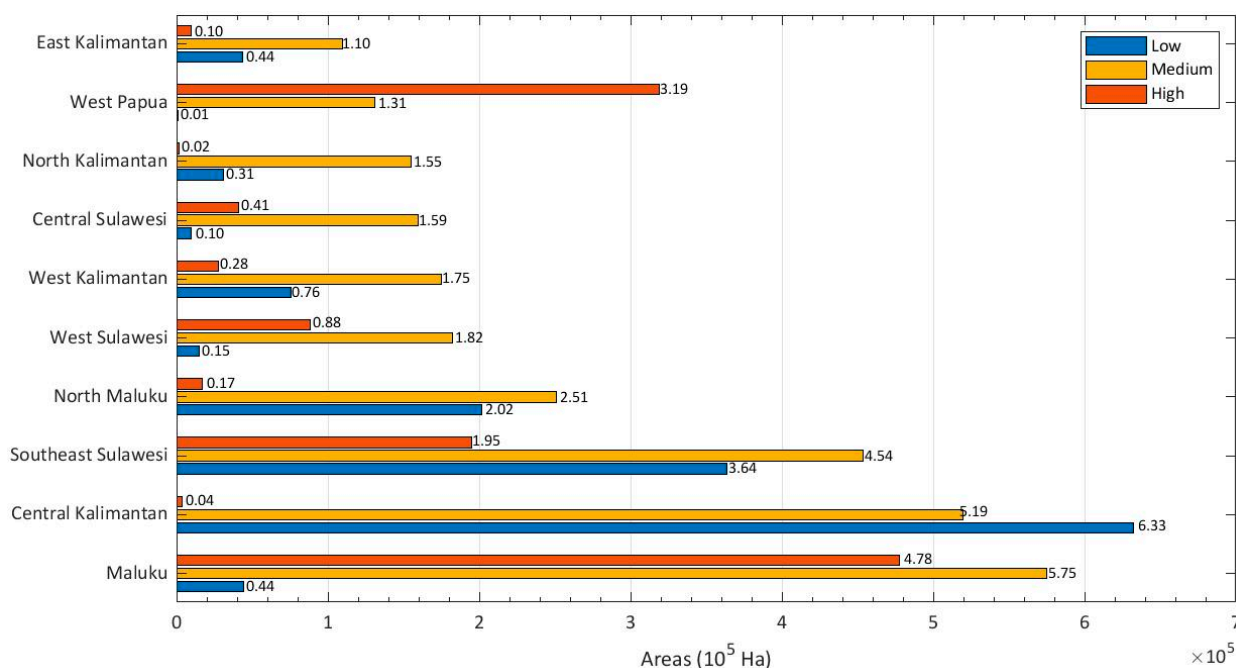
Figure 18. Top ten highest provinces in terms of highest wildfire mitigation priority areas in mining areas.

4.3. Study Limitation

This study has several limitations, including data and processing methods. In the discussed wildfire susceptibility analysis, the tropical forest data used refer to 2001, and therefore the latest data must be used in the future. In addition, vegetation types were considered homogeneous. Furthermore, the weights for each parameter were considered equivalent. For carbon stock analysis, the data products of carbon stock above- and below-ground have low spatial resolution, that is, 300 m and 500 m, respectively, leading to lower accuracy in the estimation of carbon uptake (biomass). In addition, the biomass data products used in this study used diverse data. Field validation was not carried out for air quality analysis; however, remote sensing measurements related to air quality are coherent with field data, and can represent in situ measurements [60]. The burned-area data product used for ascertaining wildfire patterns, particularly emerging hotspots, has a low resolution and cannot detect areas of <25 ha that are affected by small wildfires [61]. Land-use data for analyzing palm oil plantations and mining areas were not sourced from the government as there is no transparency in data pertaining to permits for cultivation from the Ministry of Agrarian Affairs and Spatial Planning/National Land Agency, for mining from the Ministry of Energy and Mineral Resources, for plantation business from the Ministry of Agriculture, and for timber forest product utilization from the Ministry of Environment. The problem of data disclosure affects the implementation of a one-map policy and results in the overlap between mining areas and oil-palm plantations. In addition, the analysis of forest management policies did not include the duration for the grant of permits for mining and oil-palm plantations and did not include other forest concession areas such as industrial forest plantations.

4.4. Future Research

Further research opportunities include the use of integrated tropical forest vegetation diversity data for better representativeness, use of higher-resolution data to determine carbon stock, and combining air dispersion with gas emission change pattern data for understanding dispersion trends. The following future study also can be integrated not only in regional-impact emissions (air quality: CO, NO_2, etc.), but also in global impact emissions (Greenhouse gasses: CO_2, CH_4, etc.) [62,63]. CO and CO_2 emissions are released into the atmosphere by a combustion process that affects biomass carbon release in the

air. The calculation of potential air emissions and chemical reactions between forest fire emissions is difficult to calculate and predict because the timing and location of forest fires are difficult to predict [64]. The development of a data-integration methodology by adding various other parameters and applying weighting by considering different relationships between parameters is required. In terms of accuracy assessment, a grid-based agreement level method could be adopted to assess the consistency of the result based on similar existing models [65–68]. This study can be localized using high-resolution data to examine wildfires caused by natural or human actions. From a legal perspective, analysis must be based on data from other chronological parameters, such as forest concession rights and industrial forest plantation. Moreover, it is possible to add details of forest management on national and regional scales to outline the impacts of these regulations on deforestation and, consequently, policy evaluation.

In the context of tropical rainforests management, a multi-sensor data-intensive approach could be explored to study long-term forests dynamics in the priority areas [69,70]. In addition, land-suitability analysis could be conducted to support wildfire mitigation through rehabilitation and agroforestry programs [71–74]. New trends in image processing, such as artificial intelligence methods, especially machine learning [75] and deep learning, can improve forest fire susceptibility analysis in the future [76–78]. Besides, the intensive use of data, such as climate projection and extreme precipitation, using a long-term climate model, will enhance the quality of the wildfire prediction analysis [79]. Furthermore, predictive analysis based on future climate scenarios could be studied to estimate different impacts of various wildfire mitigation strategies [80,81]. The results of this study are expected to serve as a guide in the selection of an effective area for REDD+ implementation. Wildfire priority areas identified in this study can be used for prioritizing mitigation and prevention of deforestation caused by wildfires. Deforestation patterns could also be used as information for the government in the selection of prioritized forest areas for the implementation of REDD+.

5. Conclusions

A comprehensive analysis of wildfires in Indonesia was carried out based on five aspects, including wildfire susceptibility, carbon stocks, carbon emissions, historical patterns of wildfire, and legal aspects of land use. Results showed that Sumatra and Kalimantan are highly vulnerable displaying monthly patterns that follow the climate cycle peaking between July and September. Kalimantan had the highest carbon stock in Indonesia. The highest standard deviation value was 1135.41 tons, the lowest was 1.30 tons, and the average for all regions of Indonesia was 473.51 tons. Papua and Kalimantan displayed high standard deviations and the minimum was in Java. The wildfire mitigation priority model showed that 379.516 km^2 showed a high-priority status, and they are mostly in Sumatra, Kalimantan, and North Maluku. Based on the integration of the wildfire priority model and emerging hotspots, 19.50% of the forest areas were identified as priority areas for wildfire mitigation in Indonesia. Over the last ten years, oscillating coldspot and hotspot categories were dominant, and these are found in Riau, Jambi, South Sumatra, West Kalimantan, Central Kalimantan, and Merauke. Based on legal aspects pertaining to land use, 5.2% of high-priority areas are in oil palm permit areas that are primarily found in Kalimantan, while 3.9% of high-priority areas are in mining permit areas that are mainly located in Maluku, Central Kalimantan, and Southeast Sulawesi. Overall, the results of this study provide support for technical and administrative aspects that can help policymakers to determine suitable priority areas for the implementaion of the REDD+ program and serve as a guide for the evaluation of lan—use policies in areas with high wildfire mitigation priority status.

References

1. Pawar, K.V.; Rothkar, R.V. Forest Conservation & Environmental Awareness. *Procedia Earth Planet. Sci.* **2015**, *11*, 212–215. [CrossRef]
2. Waring, R.H. Forest Ecosystems||Carbon Cycle. 2007. Available online: https://zh.booksc.eu/book/73075476/08b8ea (accessed on 7 January 2022).
3. FAO; UNEP. *The World's Forests*; FAO: Rome, Italy; UNEP: Nairobi, Kenya, 2020; ISBN 9789251324196.
4. Wicaksono, D.A.; Yurista, A.P. Konservasi Hutan Partisipatif Melalui REDD+ (Studi Kasus Kalimantan Tengah Sebagai Provinsi Percontohan REDD+). *J. Wil. Dan Lingkung.* **2013**, *1*, 189–200. [CrossRef]
5. Turubanova, S.; Potapov, P.V.; Tyukavina, A.; Hansen, M.C. Ongoing primary forest loss in Brazil, Democratic Republic of the Congo, and Indonesia. *Environ. Res. Lett.* **2018**, *13*, 074028. [CrossRef]
6. Global Forest Watch Indonesia Deforestation Rates & Statistics|GFW. Available online: https://www.globalforestwatch.org/dashboards/country/IDN/ (accessed on 19 November 2020).
7. Certini, G. Effects of fire on properties of forest soils: A review. *Oecologia* **2005**, *143*, 1–10. [CrossRef]
8. Dennis, R.; Meijaard, E.; Applegate, G.; Nasi, R.; Moore, P. *Impacts of Human-Caused Fires on Biodiversity and Ecosystem Functioning, and their Causes in Tropical, Temperate and Boreal Forest Biomes*; Secretariat of the Convention on Biological Diversity: Montreal, QC, Canada, 2001; ISBN 9280721127.
9. Jones, M.W.; Smith, A.; Betts, R.; Canadell, J.G.; Prentice, I.C.; Le Quéré, C. Climate Change increases the risk of wildfires. *Sci. Rev.* **2020**, *116*, 117.
10. Heidari, H.; Arabi, M.; Warziniack, T. Effects of Climate Change on Natural-Caused Fire Activity in Western U.S. National Forests. *Atmosphere* **2021**, *12*, 981. [CrossRef]
11. Dawud, Y. Dawud Smoke episodes and assessment of health impacts related to haze from forest fires: Indonesian experience. The Indonesian Association of Pulmonologist. *J. R. Soc. West. Aust.* **1999**, *88*, 133–138.
12. Muhammad, S.; Long, X.; Salman, M. COVID-19 pandemic and environmental pollution: A blessing in disguise? *Sci. Total Environ.* **2020**, *728*, 138820. [CrossRef] [PubMed]
13. WHO. *Ambient Air Pollution: A Global Assessment of Exposure and Burden of Disease*; World Health Organization: Geneva, Switzerland, 2016; Volume 360.
14. Reid, C.E.; Brauer, M.; Johnston, F.H.; Jerrett, M.; Balmes, J.R.; Elliott, C.T. Critical review of health impacts of wildfire smoke exposure. *Environ. Health Perspect.* **2016**, *124*, 1334–1343. [CrossRef]
15. KLHK Rekapitulasi Luas Kebakaran Hutan dan Lahan (Ha) Per Provinsi di Indonesia Tahun 2015–2020. Available online: http://sipongi.menlhk.go.id/hotspot/luas_kebakaran (accessed on 28 November 2020).
16. RENSTRA. *Peraturan Menteri Lingkungan Hidup dan Kehutanan RI No P/16/MENLHK/SETJEN/SET.1/8/2020 Tentang Rencana Strategis Kementerian Lingkungan Hidup Dan Kehutanan Tahun 2020–2024*; Kementerian Lingkungan Hidup dan Kehutanan Republik Indonesia: Jakarta, Indonesia, 2020; Volume 53, ISBN 9788578110796.
17. KLHK. *Status Hutan dan Kehutanan Indonesia 2018*; Kementerian Lingkungan Hidup dan Kehutanan Republik Indonesia: Jakarta, Indonesia, 2018; ISBN 9786028358859.
18. Erten, E.; Kurgun, V.; Musao, N. Forest Fire Risk Zone Mapping From Satellite. *Civ. Eng.* **1996**, *1*, 1–27.
19. Jaiswal, R.K.; Mukherjee, S.; Raju, K.D.; Saxena, R. Forest fire risk zone mapping from satellite imagery and GIS. *Int. J. Appl. Earth Obs. Geoinf.* **2002**, *4*, 1–10. [CrossRef]

20. Ghorbanzadeh, O.; Blaschke, T.; Gholamnia, K.; Aryal, J. Forest fire susceptibility and risk mapping using social/infrastructural vulnerability and environmental variables. *Fire* **2019**, *2*, 50. [CrossRef]

21. Ma, W.; Feng, Z.; Cheng, Z.; Chen, S.; Wang, F. Identifying forest fire driving factors and related impacts in china using random forest algorithm. *Forests* **2020**, *11*, 507. [CrossRef]

22. Baccini, A.; Goetz, S.J.; Walker, W.S.; Laporte, N.T.; Sun, M.; Sulla-Menashe, D.; Hackler, J.; Beck, P.S.A.; Dubayah, R.; Friedl, M.A.; et al. Estimated carbon dioxide emissions from tropical deforestation improved by carbon-density maps. *Nat. Clim. Chang.* **2012**, *2*, 1354. [CrossRef]

23. Spawn, S.A.; Sullivan, C.C.; Lark, T.J.; Gibbs, H.K. Harmonized global maps of above and belowground biomass carbon density in the year 2010. *Sci. Data* **2020**, *7*, 112–122. [CrossRef]

24. Soto-Navarro, C.; Ravilious, C.; Arnell, A.; De Lamo, X.; Harfoot, M.; Hill, S.L.L.; Wearn, O.R.; Santoro, M.; Bouvet, A.; Mermoz, S.; et al. Mapping co-benefits for carbon storage and biodiversity to inform conservation policy and action. *Philos. Trans. R. Soc. B Biol. Sci.* **2020**, *375*, 20190128. [CrossRef]

25. ESA Sentinel-5P TROPOMI User Guide—Sentinel Online—Sentinel. Available online: https://sentinel.esa.int/web/sentinel/user-guides/sentinel-5p-tropomi (accessed on 20 November 2020).

26. Barbosa, J.M.; Asner, G.P. Prioritizing landscapes for restoration based on spatial patterns of ecosystem controls and plant–plant interactions. *J. Appl. Ecol.* **2017**, *54*, 1459–1468. [CrossRef]

27. Etter, A.; Andrade, A.; Nelson, C.R.; Cortés, J.; Saavedra, K. Assessing restoration priorities for high-risk ecosystems: An application of the IUCN red list of ecosystems. *Land Use Policy* **2020**, *99*, 104874. [CrossRef]

28. Reddy, C.S.; Faseela, V.S.; Unnikrishnan, A.; Jha, C.S. Earth observation data for assessing biodiversity conservation priorities in South Asia. *Biodivers. Conserv.* **2019**, *28*, 2197–2219. [CrossRef]

29. Tracey, J.A.; Rochester, C.J.; Hathaway, S.A.; Preston, K.L.; Syphard, A.D.; Vandergast, A.G.; Diffendorfer, J.E.; Franklin, J.; MacKenzie, J.B.; Oberbauer, T.A.; et al. Prioritizing conserved areas threatened by wildfire and fragmentation for monitoring and management. *PLoS ONE* **2018**, *13*, e0200203. [CrossRef]

30. Raharjo, B.; Nakagoshi, N. Priorities mapping in landscape: Spatial decision support of the Indonesian forest landscape. In *Landscape Ecology for Sustainable Society*; Springer: Cham, Switzerland, 2018; pp. 155–180. [CrossRef]

31. Silva, F.R.Y.; Martínez, J.R.M.; González-Cabán, A. A methodology for determining operational priorities for prevention and suppression of wildland fires. *Int. J. Wildland Fire* **2014**, *23*, 544–554. [CrossRef]

32. Irwansyah Fauzi, A.; Dimara Sakti, A.; Fajri Yayusman, L.; Budi Harto, A.; Budi Prasetyo, L.; Irawan, B.; Wikantika, K. Evaluating mangrove forest deforestation causes in Southeast Asia by analyzing recent environment and socio-economic data products. In Proceedings of the 39th Asian Conference on Remote Sensing Enabling Prosper ACRS 2018, Kuala Lumpur, Malaysia, 15–19 October 2018; Volume 2, pp. 880–889.

33. Fauzi, A.; Sakti, A.; Yayusman, L.; Harto, A.; Prasetyo, L.; Irawan, B.; Kamal, M.; Wikantika, K. Contextualizing mangrove forest deforestation in southeast asia using environmental and socio-economic data products. *Forests* **2019**, *10*, 952. [CrossRef]

34. Sakti, A.D.; Rinasti, A.N.; Agustina, E.; Diastomo, H.; Muhammad, F.; Anna, Z.; Wikantika, K. Multi-scenario model of plastic waste accumulation potential in indonesia using integrated remote sensing, statistic and socio-demographic data. *ISPRS Int. J. Geo-Inf.* **2021**, *10*, 481. [CrossRef]

35. Xu, Y.; Mo, Y.; Zhu, S. Poverty mapping in the dian-gui-qian contiguous extremely poor area of southwest china based on multi-source geospatial data. *Sustainability* **2021**, *13*, 8717. [CrossRef]

36. Chen, C.; He, X.; Liu, Z.; Sun, W.; Dong, H.; Chu, Y. Analysis of regional economic development based on land use and land cover change information derived from Landsat imagery. *Sci. Rep.* **2020**, *10*, 12721. [CrossRef]

37. Sakti, A.D.; Fauzi, A.I.; Wilwatikta, F.N.; Rajagukguk, Y.S.; Sudhana, S.A.; Yayusman, L.F.; Syahid, L.N.; Sritarapipat, T.; Principe, J.A.; Quynh Trang, N.T.; et al. Multi-source remote sensing data product analysis: Investigating anthropogenic and naturogenic impacts on mangroves in southeast asia. *Remote Sens.* **2020**, *12*, 2720. [CrossRef]

38. Fauzi, A.I.; Sakti, A.D.; Robbani, B.F.; Ristiyani, M.; Agustin, R.T.; Yati, E.; Nuha, M.U.; Anika, N.; Putra, R.; Siregar, D.I.; et al. Assessing potential climatic and human pressures in indonesian coastal ecosystems using a spatial data-driven approach. *ISPRS Int. J. Geo-Inf.* **2021**, *10*, 778. [CrossRef]

39. Sakti, A.D.; Ario, M.; Rahadianto, E.; Pradhan, B.; Muhammad, H.N.; Andani, I.G.A.; Sarli, P.W.; Abdillah, M.R.; Anggraini, T.S.; Purnomo, A.D.; et al. School Location Analysis by Integrating the Accessibility, Natural and Biological Hazards to Support Equal Access to Education. *ISPRS Int. J. Geo-Inf.* **2021**, *11*, 12. [CrossRef]

40. BIG Indonesia Geospatial Portal. Available online: https://tanahair.indonesia.go.id/portal-web (accessed on 19 November 2020).

41. CSM Earth Observation Goup. Available online: https://eogdata.mines.edu/products/vnl/ (accessed on 20 August 2021).

42. NASA LP DAAC—MOD11A1. Available online: https://lpdaac.usgs.gov/products/mod11a1v006/ (accessed on 18 May 2021).

43. WorldPop Open Spasial Demographic Data and Research. Available online: https://www.worldpop.org/ (accessed on 20 November 2020).

44. Funk, C.; Peterson, P.; Landsfeld, M.; Pedreros, D.; Verdin, J.; Shukla, S.; Husak, G.; Rowland, J.; Harrison, L.; Hoell, A.; et al. The climate hazards infrared precipitation with stations—A new environmental record for monitoring extremes. *Sci. Data* **2015**, *2*, 150066. [CrossRef]

45. Takeuchi, W.; Darmawan, S.; Shofiyati, R.; Khiem, M.V.; Oo, K.S.; Pimple, U.; Heng, S. Near-real time meteorological drought monitoring and early warning system for croplands in Asia. In Proceedings of the ACRS 2015—Asian Conference on Remote Sensing 2015: Fostering Resilient Growth in Asia, Metro Manila, Philippines, 24–28 October 2015.

46. ECMWF Copernicus Climate Change Service (C3S). ERA5: Fifth generation of ECMWF atmospheric reanalyses of the global climate. *Copernic. Clim. Change Serv. Clim. Data Store* **2017**. Available online: https://cds.climate.copernicus.eu/cdsapp#!/home (accessed on 10 August 2020).

47. Weiss, D.J.; Nelson, A.; Gibson, H.S.; Temperley, W.; Peedell, S.; Lieber, A.; Hancher, M.; Poyart, E.; Belchior, S.; Fullman, N.; et al. A global map of travel time to cities to assess inequalities in accessibility in 2015. *Nature* **2018**, *553*, 333–336. [CrossRef] [PubMed]

48. Hansen, M.C.; Potapov, P.V.; Moore, M.; Hancher, S.A.; Turubanova, A.; Tyukavina, D.; Thau, S.V.; Stehman, S.J.; Goetz, T.R.; Loveland, A.; et al. High-resolution global maps of 21st-century forest cover change. *Science* **2013**, *850*, 2011–2014. [CrossRef] [PubMed]

49. Pettinari, M.L.; Lizundia-Loiola, J.; Chuvieco, E. ESA CCI ECV Fire Disturbance: D4.2 Product User Guide—MODIS, Version 1.0; 2020. Available online: https://www.esa-fire-cci.org/documents (accessed on 18 May 2021).

50. Giglio, L.; Boschetti, L.; Roy, D.; Hoffman, A.A.; Humber, M. Collection 6 MODIS Burned Area product User Guide. *Nasa* **2016**, *3*, 1–26.

51. FWI Konsesi Perusahaan. Available online: https://petahutan.fwi.or.id/web/map/name/konsesiperusahaan (accessed on 20 November 2020).

52. Misra, P.; Fujikawa, A.; Takeuchi, W. Novel decomposition scheme for characterizing urban air quality with MODIS. *Remote Sens.* **2017**, *9*, 812. [CrossRef]

53. Hennig, C.; Viroli, C. Quantile-based classifiers. *Biometrika* **2016**, *103*, 435–446. [CrossRef] [PubMed]

54. Esri How Emerging Hot Spot Analysis works—ArcGIS Pro | Documentation. Available online: https://pro.arcgis.com/en/pro-app/latest/tool-reference/space-time-pattern-mining/learnmoreemerging.htm (accessed on 26 April 2021).

55. Kurniawan, A.; Sadali, M.I. Pemanfaatan Analisis Spasial Hot Spot (Getis Ord Gi*) untuk Pemetaan Klaster Industri di Pulau Jawa dengan Memanfaatkan Sistem Informasi Geografi. *OSF Preprints* **2020**, *1*, 1–21. [CrossRef]

56. Pribadi, A.; Kurata, G. Greenhouse gas and air pollutant emissions from land and forest fire in Indonesia during 2015 based on satellite data. In Proceedings of the IOP Conference Series: Earth and Environmental Science, Bogor, Indonesia, 25–26 October 2016; Volume 54.

57. BPS Badan Pusat Statistik. Available online: https://www.bps.go.id/indicator/12/141/1/kepadatan-penduduk-menurut-provinsi.html (accessed on 19 November 2020).

58. KLHK Data Matrix Titik Panas TERRA/AQUA (LAPAN). Available online: http://sipongi.menlhk.go.id/hotspot/matrik_tahunan?satelit=LPN-MODIS&thn=2019 (accessed on 20 November 2020).

59. LAPAN LAPAN Fire Hotspot. Available online: http://modis-catalog.lapan.go.id/monitoring/ (accessed on 19 August 2021).

60. Zheng, Z.; Yang, Z.; Wu, Z.; Marinello, F. Spatial variation of NO2 and its impact factors in China: An application of sentinel-5P products. *Remote Sens.* **2019**, *11*, 1939. [CrossRef]

61. Miettinen, J. *Burnt Area Mapping in Insular Southeast Asia Using Medium Resolution Satellite Imagery*; Dissertationes Forestales: Helsinki, Finlandia, 2007; Volume 2007, ISBN 9789516511781.

62. Carvalho, A.; Monteiro, A.; Flannigan, M.; Solman, S.; Miranda, A.I.; Borrego, C. Forest fires in a changing climate and their impacts on air quality. *Atmos. Environ.* **2011**, *45*, 5545–5553. [CrossRef]

63. Sastry, N. Forest fires, air pollution, and mortality in Southeast Asia. *Demography* **2002**, *39*, 1–23. [CrossRef]

64. de Gouw, J.A.; Warneke, C.; Stohl, A.; Wollny, A.G.; Brock, C.A.; Cooper, O.R.; Holloway, J.S.; Trainer, M.; Fehsenfeld, F.C.; Atlas, E.L.; et al. Volatile organic compounds composition of merged and aged forest fire plumes from Alaska and western Canada. *J. Geophys. Res. Atmos.* **2006**, *111*, 1–20. [CrossRef]

65. Sakti, A.D.; Takeuchi, W.; Wikantika, K. Development of Global Cropland Agreement Level Analysis by Integrating Pixel Similarity of Recent Global Land Cover Datasets. *J. Environ. Prot.* **2017**, *8*, 1509–1529. [CrossRef]

66. Herold, M.; Mayaux, P.; Woodcock, C.E.; Baccini, A.; Schmullius, C. Some challenges in global land cover mapping: An assessment of agreement and accuracy in existing 1 km datasets. *Remote Sens. Environ.* **2008**, *112*, 2538–2556. [CrossRef]

67. Lu, M.; Wu, W.B.; Zhang, L.; Liao, A.P.; Peng, S.; Tang, H.J. A comparative analysis of five global cropland datasets in China. *Sci. China Earth Sci.* **2016**, *59*, 2307–2317. [CrossRef]

68. Rajagukguk, Y.S.; Sakti, A.D.; Yayusman, L.F.; Harto, A.B.; Prasetyo, L.B.; Irawan, B.; Wikantika, K. Evaluation of Southeast Asia mangrove forest deforestation using longterm remote sensing index datasets. In Proceedings of the 39th Asian Conference on Remote Sensing: Remote Sensing Enabling Prosperity, ACRS 2018, Kuala Lumpur, Malaysia, 15–19 October 2018; Asian Association on Remote Sensing: Kuala Lumpur, Malaysia, 2018; Volume 2, pp. 931–937.

69. Sakti, A.D.; Takeuchi, W. A data-intensive approach to address food sustainability: Integrating optic and microwave satellite imagery for developing long-term global cropping intensity and sowing month from 2001 to 2015. *Sustainability* **2020**, *12*, 3227. [CrossRef]

70. Decuyper, M.; Chávez, R.O.; Lohbeck, M.; Lastra, J.A.; Tsendbazar, N.; Hackländer, J.; Herold, M.; Vågen, T.G. Continuous monitoring of forest change dynamics with satellite time series. *Remote Sens. Environ.* **2022**, *269*, 112829. [CrossRef]

71. Nath, A.J.; Kumar, R.; Devi, N.B.; Rocky, P.; Giri, K.; Sahoo, U.K.; Bajpai, R.K.; Sahu, N.; Pandey, R. Agroforestry land suitability analysis in the Eastern Indian Himalayan region. *Environ. Chall.* **2021**, *4*, 100199. [CrossRef]

72. Ahmad, F.; Uddin, M.M.; Goparaju, L.; Rizvi, J.; Biradar, C. Quantification of the Land Potential for Scaling Agroforestry in South Asia. *KN-J. Cartogr. Geogr. Inf.* **2020**, *70*, 71–89. [CrossRef]

73. Özkan, B.; Dengiz, O.; Turan, İ.D. Site suitability analysis for potential agricultural land with spatial fuzzy multi-criteria decision analysis in regional scale under semi-arid terrestrial ecosystem. *Sci. Rep.* **2020**, *10*, 22074. [CrossRef]

74. Sakti, A.D.; Tsuyuki, S. Spectral Mixture Analysis of Peatland Imagery for Land Cover Study of Highly Degraded Peatland in Indonesia. In *The International Archives of the Photogrammetry, Remote Sensing and Spatial Information Science*; Copernicus Publications: Göttingen, Germany, 2015; Volume XL-7/W3.

75. Jain, P.; Coogan, S.C.P.; Subramanian, S.G.; Crowley, M.; Taylor, S.; Flannigan, M.D. A review of machine learning applications in wildfire science and management. *Environ. Rev.* **2020**, *28*, 478–505. [CrossRef]

76. Monaco, S.; Greco, S.; Farasin, A.; Colomba, L.; Apiletti, D.; Garza, P.; Cerquitelli, T.; Baralis, E. Attention to Fires: Multi-Channel Deep Learning Models for Wildfire Severity Prediction. *Appl. Sci.* **2021**, *11*, 11060. [CrossRef]

77. Guede-Fernández, F.; Martins, L.; de Almeida, R.V.; Gamboa, H.; Vieira, P. A Deep Learning Based Object Identification System for Forest Fire Detection. *Fire* **2021**, *4*, 75. [CrossRef]

78. Saponara, S.; Elhanashi, A.; Gagliardi, A. Real-time video fire/smoke detection based on CNN in antifire surveillance systems. *J. Real-Time Image Proc.* **2021**, *18*, 889–900. [CrossRef]

79. Wang, B.; Waters, C.; Anwar, M.R.; Cowie, A.; Liu, D.L.; Summers, D.; Paul, K.; Feng, P. Future climate impacts on forest growth and implications for carbon sequestration through reforestation in southeast Australia. *J. Environ. Manag.* **2022**, *302*, 113964. [CrossRef] [PubMed]

80. Syahid, L.N.; Sakti, A.D.; Virtriana, R.; Wikantika, K.; Windupranata, W.; Tsuyuki, S.; Caraka, R.E.; Pribadi, R. Determining optimal location for mangrove planting using remote sensing and climate model projection in southeast asia. *Remote Sens.* **2020**, *12*, 3734. [CrossRef]

81. Yospin, G.I.; Bridgham, S.D.; Neilson, R.P.; Bolte, J.P.; Bachelet, D.M.; Gould, P.J.; Harrington, C.A.; Kertis, J.A.; Evers, C.; Johnson, B.R. A new model to simulate climate-change impacts on forest succession for local land management. *Ecol. Appl.* **2015**, *25*, 226–242. [CrossRef]